INTEGRATED RESERVOIR MODELLING AND SIMULATION TO DETERMINE THE POTENTIAL OF SHALE GAS: A South African context

MSc (50/50) RESEARCH REPORT

Prepared by

Ramasela Theresa Rammutla
730244

Submitted to

School of Chemical and Metallurgical Engineering, Faculty of Engineering and Built Environment, University of the Witwatersrand, Johannesburg, South Africa, in partial fulfilment of the requirements for the degree of Master of Science in Engineering

Supervisors:
Prof. D.B. Nkazi
Dr. S. Scheiber-Enslin

Johannesburg, 2021

DECLARATION

I, **Ramasela Theresa Rammutla** declare that this research report is my own unaided work except where it is stated otherwise in the references. It is submitted in partial fulfilment of the requirements for the degree of Master of Science in Chemical Engineering (Petroleum) to the University of the Witwatersrand, Johannesburg, in the year 2021. It has not been submitted before for any degree or examination in this or any other University.

____

Signed on the **14th** day of **JUNE** 2021

ABSTRACT

The lower Ecca Group of the Karoo Basin, most notably the Whitehill Formation is believed to host shale gas. The initial exploration for oil and gas in the Karoo Basin was undertaken by the Southern Oil Exploration Corporation (Pty. Ltd.) (SOEKOR) in the 1960s, to prove/disprove the existence of economic occurrences of oil in South Africa. Since then, only limited studies have been carried out on the gas production potential of the basin.

3D reservoir modelling has become a fundamental tool in the lifecycle of hydrocarbon plays. It has formed the basis of understanding reservoir heterogeneity, volumetric calculations of hydrocarbons and field development planning. This study applies 3D Geocellular reservoir modelling carried out in Schlumberger's Petrel® Software to three boreholes drilled by SOEKOR in the Karoo Basin of South Africa, to analyse the reservoir potential. Two intervals (Top Ecca Group to Top Whitehill Formation, and Whitehill and Prince Albert Formations) were selected for this study. Using recovery factors of 30%, 75%, and 90%, new resource estimates of the two horizons are presented, namely 43 - 128 Tcf (average 107 Tcf) and 13 - 40 Tcf (average 33 Tcf), respectively. This study can be used as a basis for future improvements of the modelling workflow if new data become available in the basin.

Keywords: Karoo Basin, Whitehill Formation, 3D reservoir modelling

DEDICATION

To Nkwetsimo,

the Splendour of God’s glory

ACKNOWLEDGEMENTS

I would like to express my deepest gratitude to my supervisors, Dr Nkazi and Dr Scheiber-Enslin. Without you, this journey would not have been what it has been.

Prof Nkazi, thank you for always helping with what was needed for this research, ensuring that I always had what I needed and for your encouragement to aim for better. Your heart is really appreciated.

To Dr Scheiber-Enslin, it has been a delight working with you. Thank you so much for giving of your time, resources and knowledge.

I thank the Petroleum Agency South Africa for access to the SOEKOR borehole data. Sean Johnson and Selwyn Adams are thanked greatly for their guidance and assistance.

I would also like to extend many thanks to Prof Musa Manzi of the Seismic Research Centre, School of Geosciences for opening the doors to the centre for me to use their resources when I needed to.

Nathi, thank you for your never-ending support and words of encouragement during the times when I thought I could no longer carry on with this research.

Glory be to the Risen King, now and forever!

TABLE OF CONTENTS

List of Figures

List of Tables

Nomenclature

Gas Initially In place (GIIP) - refers to an estimate of the total amount of gas that is contained/trapped within shale rock.

Technically Recoverable Reserves (TRR) - refers to the estimated amount of shale gas that might be technically recovered if there are no constraints on production, such as economics.

CHAPTER ONE

INTRODUCTION

1.1 BACKGROUND AND MOTIVATION

Shale gas reservoirs have reshaped the global energy market over the years owing not only to the increase in global energy demand and declining energy sources but also to the improved efficiency in drilling and production of the resources. This has been brought about by the application of fractural stimulation technology, which has greatly increased the ability to profitably produce shale gas (Mohaghegh, 2011; Mohaghegh et al., 2012; U.S. Energy Information (EIA), 2011; Wang and Carr, 2013). With increasing industrialization, not only in South Africa but globally as well, the need to exploit these shale gas reservoirs becomes pertinent. The world has seen a rapid increase in shale gas production in China and America, though not in other countries, specifically South Africa. This study uses 3D Geocellular Modelling to evaluate the shale gas potential of the Karoo Basin of South Africa. This allowed for reserve estimates to be made, which has an impact on the production of the hydrocarbon play.

Shale rocks are fine-grained, generally dark coloured and organic-rich sedimentary rocks. In a petroleum system there are four basic requirements to be met for the subsurface accumulation of hydrocarbon reserves i.e (1) source rock/s; (2) migration pathway away from the source rock; (3) reservoirs into which the expelled hydrocarbons migrate; and (4) a trapping mechanism (Aplin, 2000; CSIR, 2016; Selley, 1998). During the maturation of the organic matter contained in shale rocks, natural gas (termed shale gas) is generated (Chere et al., 2017; de Kock et al., 2017). Shale rocks are termed unconventional as the gas generated is retained within the shale which acts as the source rock, reservoir, seal and trap (Wopara, 2018; Wright et al., 2015). The classification of unconventional reserves is not simply restricted to geology, but factors such as the cost to develop the reserve play a significant role (CSIR, 2016).

Shale gas is natural gas that consists mainly of methane (methane is the primary component in the gas, typically 80% or more with other smaller quantities of gas) that is trapped in formations of low permeability and low porosity. The gas in the shale formations flows out during the application of hydraulic fracturing. Shale gas is generated from organic matter and stored in shale source rocks in different ways **(Figure 1.1)**: (1) primarily as adsorbed on the surface of clays and organics; (2) dissolved in the kerogen or bitumen; (3) and as free gas in pore spaces or within the fracture network (Chere et al., 2017; CSIR, 2016; Dahaghi and Mohaghegh, 2011; de Kock et al., 2017; Jarvie et al., 2007; Muntendam-Bos et al., 2009; Zhang et al., 2018).

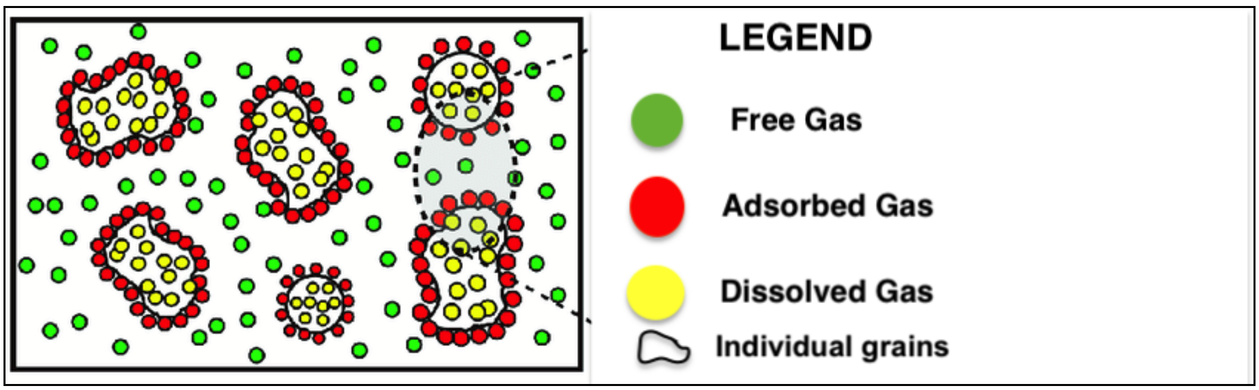

Figure 1.1. Storage forms of shale gas in shale source rocks (modified after Zhang et al., 2018).

The process of adsorption plays a significant role in the determination of the final product in the petroleum system (Pepper, 1991). Accordingly, desorbed gas (refers to the gas that is released from the surface of the grains when the pressure changes, either increasing or decreasing) can probably be ignored when doing the initial performance evaluation of the well, as it usually only adds about 5-15% of the ultimate gas recovered. The amount of gas that is found in place is influenced, amongst other things, by the degree of thermal maturation of the organic matter in the rocks. In the Karoo Basin of South Africa, the degree of thermal maturation is said to be higher due to the tectonic events that led to the emplacement of igneous intrusions (Chere et al., 2017).

Unconventional systems also depend highly on fracture permeability of the rocks, which may be natural or stimulated for production (Jarvie et al., 2007). Natural fractures play a significant role in gas production as they are the primary conduit of permeability in the reservoir. The fractures are influenced by organic matter decomposition and/or tectonic processes (Jarvie et al., 2007). The success of hydraulic fracturing is greatly increased when it intersects the existing natural fractures in the shale.

It is commonly a challenge to map the extent and distribution of these fractures, even with advanced techniques (Mohaghegh, 2011; Mohaghegh et al., 2012). There is also a level of uncertainty in matrix permeability and complexity of fractures, making it difficult to model production in unconventional gas reservoirs (Dahaghi and Mohaghegh, 2011).

The main challenge encountered with the production of unconventional reservoirs is the very small pore size, and very low matrix permeability of the source rock (Labed, Oyeneyin and Oluyemi, 2018; Lijun et al., 2019). Hydraulic fracturing of the rock becomes necessary to obtain commercial amounts of gas by increasing the permeability of the matrix (Sunjay, Kumar, and Jain, 2014). This is done in order to enhance the flow of hydrocarbons from the rocks. The process typically involves drilling vertical and horizontal sections through which highly pressured fluid is pumped into the target formation **(Figure 1.2)**. The fractures are usually kept open by sand particles that are incorporated into the fluid (CSIR, 2016; USGS, 2019; Yew, 2017). The success of hydraulic fracturing is greatly increased when it intersects the existing natural fractures in the shale.

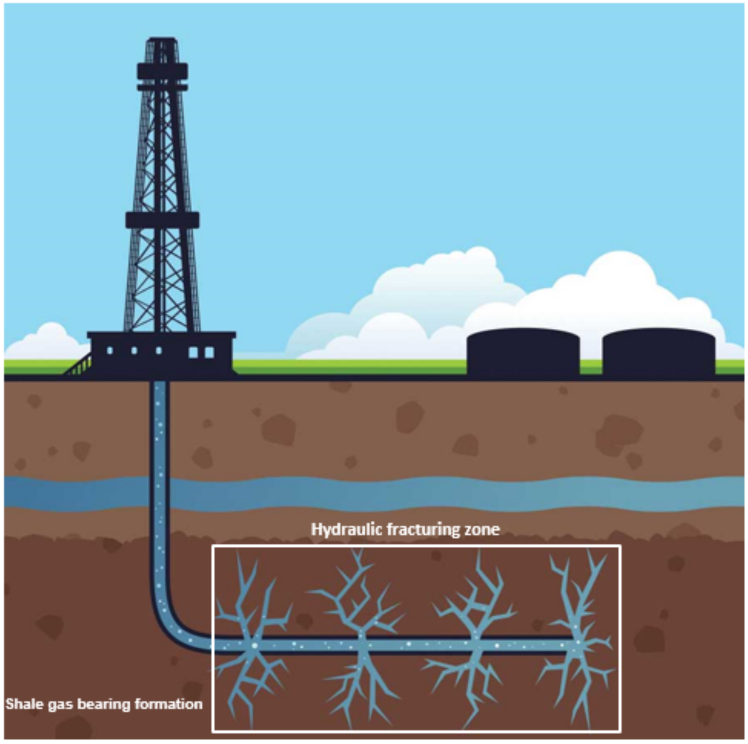

Figure 1.2. Image showing the process of hydraulic fracturing and the propagation of induced fractures (modified after Motherearthnews.com, 2012).

Energy companies invest money in exploring and developing these reservoirs, therefore a good understanding of the geology and transport characteristics of shale gas is important in the development of the reservoir and in improving the efficiency at which the gas is extracted. As a result, an understanding of how the gas flows within these reservoirs is paramount for the successful development and extraction of the gas.

Comprehensive geological and geophysical studies have been undertaken in the Karoo over the years to evaluate the igneous intrusions in the basin. The occurrence of these intrusions, mainly dolerite dykes and sills, in the major prospective area need to be taken into consideration in any future development and study plans. The aim of this study is to incorporate those studies and their findings to estimate the amount of gas in place also considering changing variables. To evaluate the feasibility of the economic production of shale gas, it is important that modelling of the reservoir be undertaken.

Studies on the modelling of gas flow in unconventional reservoirs have been conducted in North America and China. This study will focus on gas reserve estimates in a South African context by establishing a static 3D geological model and a dynamic reservoir model with simulation.

1.2 AIM AND OBJECTIVES OF STUDY

The aim of this study was to create a static and dynamic geological model populated with borehole and core data. The static model in this study refers to the rigid, visual 3D model, and the dynamic model refers to the static 3D model as it changes over time with changing parameters. This was done so that a customized workflow that can be applied to similar scenarios can be established. The model was used to do a reserve estimate analysis of shale gas in the Karoo Basin which was then compared to results published by other workers. The results obtained from the volumetric analysis have an impact on the possible hydrocarbon exploration and development of shale gas in the Karoo Basin. The research aim was achieved in the objectives viz:

- Establishing a geological model and running reservoir simulations using Schlumberger's Petrel® software;
- Studying the effect of changing reservoir variables (porosity and gas saturation) on gas volumes using the established model;
- Determining the Gas Initially In Place (GIIP) and technically recoverable reserves (TRR); and
- Validating the established model and estimates using published data from the literature.

1.3 REPORT STRUCTURE

This report is divided into five chapters. **Chapter 1** highlights the fundamentals of shale gas and the objectives of the study. **Chapter 2** presents the history of exploration in the Karoo Basin and global parameters used in the assessment of hydrocarbon plays. This chapter also provides a review of the theory of 3D Geocellular modelling. **Chapter 3** describes the methodology and workflow used to carry out this study. The results of the study are presented in **Chapter 4**, which also includes the comparison to previous assessment studies in the Karoo Basin, and discussion of the results. The conclusions thereof are summarised in **Chapter 5**. This chapter also includes the recommendations for further studies.

CHAPTER TWO

LITERATURE REVIEW

2.1 THE HISTORY OF EXPLORATION IN THE KAROO

The Main Karoo basin of South Africa is a large erosional remnant that covers nearly two-thirds of the South African land surface and records a vast range of depositional environments that span over a century (Johnson et al., 1996; Smith, 1990). Its stratigraphy and development is a well-known subject of research conducted by several workers over the years, which is not of discussion in this study. The extensive network of dolerite intrusions occurring at various locations in the succession is part of this stratigraphy **(Figure 2.1)**.

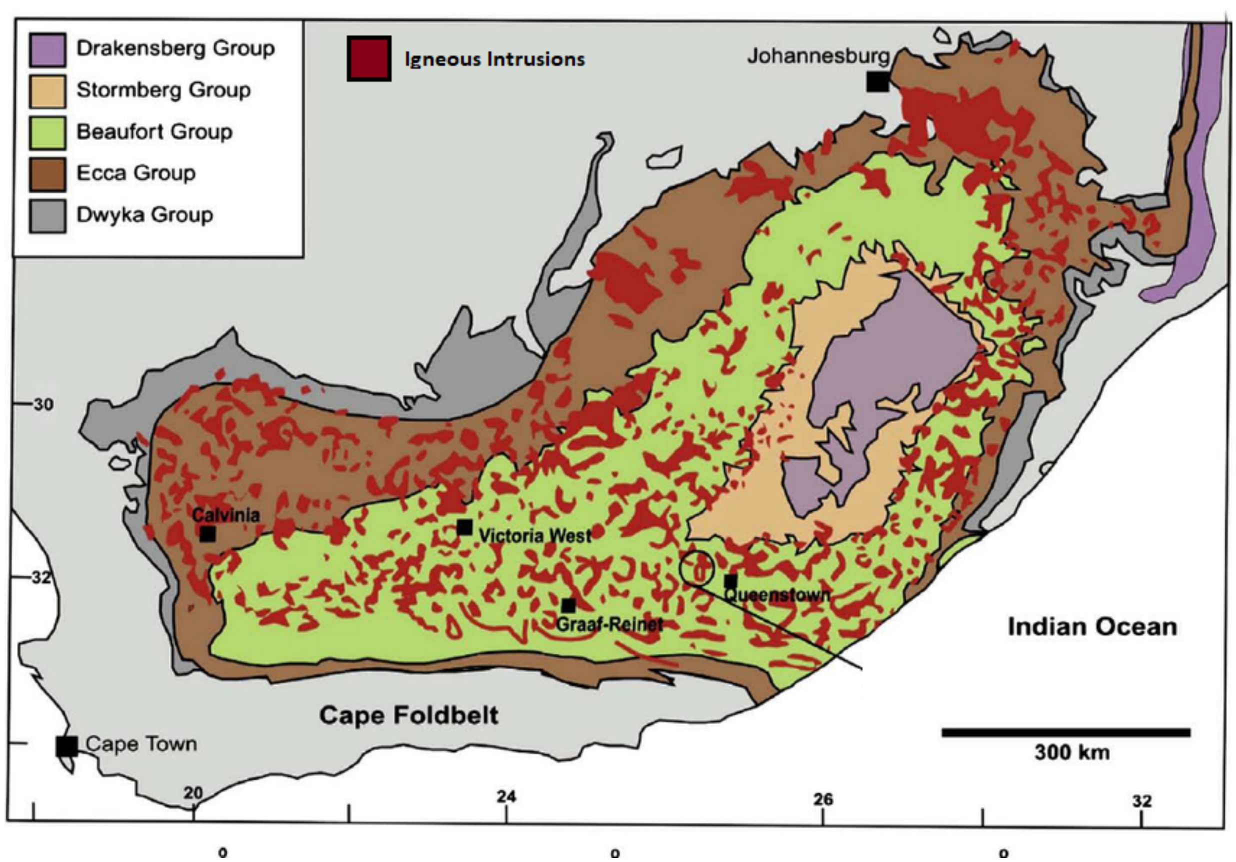

Figure 2.1. Map showing the Karoo Basin of South Africa, with igneous intrusions (modified after Aarnes, Podladchikov and Neumann, 2008).

The lower Ecca Group of the Karoo Basin, mostly the Whitehill Formation is believed to have the potential to bear shale gas at 211 Tcf (Chere et al., 2017; De Kock et al., 2017; Geel et al., 2013; U.S EIA, 2013). This primarily uses the thickness of the formation and total organic content (TOC) of the shale, based on global benchmarks such as the Marcellus shale and Barnett shale.

The first studies on hydrocarbons were conducted in the 1960s - 1970s by the then Southern Oil Exploration Corporation (SOEKOR) (now PetroSA) and were later abandoned with the perception that the potential for the development of the gas plays was low (PetroSA, 2012). With the advancement in drilling technology and the growth spurt in global shale gas development, the Karoo Basin once again became a target for exploration.

Based on the available data, it is believed that there is a potential for shale gas occurrence. The Whitehill Formation is of particular interest because of the organic-rich, thermally mature shales that make up this formation (U.S. Energy Information Administration (EIA), 2011). There are however complexities surrounding this gas play, including that the Karoo Basin is a complex structural area as it has been affected by the Cape orogeny and the emplacement of igneous bodies (Drakensberg lavas and dolerite sills and dykes) after basin closure (CSIR, 2016; de Kock et al., 2017; Scheiber-Enslin, Webb and Ebbing, 2014).

Since the initial discovery and exploration, further studies have been carried out. The aim was to demonstrate whether the shale contains gas or whether it has been thermally matured beyond a point of recovery. These studies have shown that the initial findings and preliminary studies that estimate the recoverable gas amounts to be in the ranges of 30 to 500 trillion cubic feet (Tcf) have been inflated. The recent studies on the Karoo Basin report that the actual available gas is lower, lying within the ranges of 10 to 172 Tcf with the potential of 13 Tcf being realistic (Aarnes et al., 2011; Chere et al., 2017; Cole, 2014; Decker, 2011; Decker and Marot, 2012; de Kock et al., 2017; Geel et al., 2013; Geel et al., 2015; Kuuskraa et al., 2011; Nolte et al., 2019; PetroSA, 2012).

2.2 HYDROCARBON RESERVE ANALYSIS

2.2.1 Lithological, Petrophysical, and Geochemical parameters

When evaluating shale gas plays, it is important to take into account the petrophysical properties that may affect the transport and gas storage capacity (Nolte et al., 2019). The estimation of gas flow rates can then be done with the integration of the total generation potential and thickness of the source rock, and the natural and induced fracture network (Jarvie et al., 2007).

There are various global parameters and criteria which have been developed to determine the potential of a basin to produce hydrocarbons. It is understood that the suitability of the shale for shale gas extraction depends on multiple parameters, which include amongst others the organic matter that makes up the rock. These parameters are briefly discussed below as they play(ed) a significant role in the hydrocarbon potential studies of the Karoo Basin (Baiyegunhi et al., 2019; Chere et al., 2017; Cole, 2012; de Kock et al., 2017; Jarvie et al., 2007; Jarvie, 2012; Muntendam-Bos et al., 2009; Nolte et al., 2019; Schwarzkopf, 1992; Steyl, van Tonder and Chevallier, 2012).

These parameters are important for basin analysis which characterizes the depth and thickness of the source rocks, as well as their environment of deposition and the pressure and thermal history.

- **Porosity and permeability**

  Porosity is a measure of empty spaces in the rock which can be occupied with oil, gas, or water. Permeability is the ability of the fluids to flow within the rock. These two parameters play an important role in any hydrocarbon play. The favourable values are between 4 and 7%, and <0.001 mD for porosity and permeability, respectively. The porosity values in the Karoo Basin are between 0 and 4%, whilst permeability is 0 mD (Rowsell and de Swardt, 1976).

- **Kerogen type**

  Kerogen is insoluble naturally occurring organic matter which forms during the burial and heating of organic shale. When continually buried and heated to suitable depths and temperature, the kerogen releases hydrocarbons. The initiation of the maturation of kerogen to oil occurs at temperatures of 100-150 ^{0}C, which correspond to depths of 3-4 km. A variety of organic materials make up kerogen, which include algae, wood, and pollen.

  Type I kerogen consists mainly of algae and is highly likely to produce oil. Type II consists of mixed terrestrial and marine organic matter and is likely to generate both oil and gas. Type III consists of woody terrestrial organic matter that typically generates gas. Type IV is usually not of interest as it has no capacity to generate hydrocarbons. The different types of kerogen have varying amounts of hydrogen relative to carbon and oxygen. This is the controlling factor for oil versus gas ratios.
  The type of kerogen then determines the type of hydrocarbon and the gas occurrence properties. From global references to shale gas plays in the USA and Canada, type II kerogen is the minimum favourable for the plays. The Collingham and Whitehill Formations have been observed to be type II sediments while the Prince Albert Formation is mainly type III (Geel, 2013).

- **Organic richness (Total Organic Carbon (TOC))**

  It provides a way to quantitatively estimate the volume of hydrocarbons that can be generated by the source rock depending on the kerogen type. It also controls the volume of adsorbed gas in the rock. The value needs to be at least 1%, with >2% considered to be a reasonably good source rock. From various samples, TOC values in the Karoo basin are at an average of 4.5%, with a minimum of <0.5% (Council for Geoscience, 2016; Geel et al., 2013; Rowsell and de Swardt, 1976). Increasing TOC correlates with increasing amounts of adsorbed and free gas. It becomes a challenge to determine original values in areas where you have high thermal maturity of the source rocks.

- **Thermal maturity: vitrinite reflectance and organic matter conversion**

  Vitrinite reflectance is the most commonly used parameter to determine the thermal maturity of a source rock, with favourable values ranging from ~1.25% to 2.5%. This in turn provides an indication of Tmax, which is the maximum temperature that was reached by the source rock. The thermal maturity becomes fully useful when it is directly related to the degree of organic matter conversion, which eventually relates to the preservation of hydrocarbons.

  The degree to which kerogen is converted can be determined by calculating the kerogen transformation ratio. It becomes vital that the maturity lies within the gas window. The gas window is defined by vitrinite reflectance values between 2 and 5%, with values >3.5% considered to be overmature for the economic recovery of gas. For the Karoo, it is an average of 4%, with a minimum of 1% (de Kock et al., 2017; Geel et al., 2013).

- **Mineralogy**

  This parameter becomes an important factor in tight shale systems where stimulation is required. High brittleness which is influenced by the mineralogy, is directly related to greater amounts of gas flow during fractural stimulation. Formations with high silica (quartzitic minerals) content greater than 30% become favourable due to the brittle nature of the mineral. From mineralogical analyses in the Karoo, the quartz content is within the ranges of 18-31% (Baiyegunhi et al., 2019).

- **Kubler Index (Illite Crystallinity Index)**

  The Kubler index relates to the degree of metamorphism of very low grade metamorphosed sedimentary rocks. This allows the designation of metamorphic facies and inference of the temperature at which the rock formed. Kubler index values in the Karoo basin are said to reveal a north to south increase of burial maturity, which can be attributed to the folding in the Cape Fold Belt. Lower values (~2.5 - 3) marking the onset of metamorphic conditions are observed in the south, correlating with the theory that the dolerite intrusions will have metamorphosed the sediments.

- **Rock-Eval pyrolysis and Hydrogen Index**

  The parameter is used to quantify the relative hydrogen content in the organic matter and the thermal maturity thereof. It is used as an indicator of the hydrocarbon generative capacity of the kerogen in the source rock. Hydrogen index values in the Karoo basin are very low suggesting low production potential currently.

In this study we will carry out a simple study that focuses on the porosity of the basin in the selected wells.

2.2.2 Reservoir modelling

3D Geocellular modelling

Reservoir modelling integrates multidisciplinary data and geological knowledge to create a robust representation of the subsurface (Dubrule, 1998; Oloo and Xie, 2018). The data may include geological maps, structural and seismic data, and boreholes. Model precision increases as more data are incorporated, giving a clear and detailed picture of a reservoir (Mosavel and Musekiwa, 2016; Marinovska, 2017).

The spatial variability of data across the reservoir needs to be considered when building the model. This is where geostatistical data plays a major role, maintaining a practical representation of the reservoir (Dubrule, 1998; Pro.arcgis.com, 2019). Building 3D geocellular models using geostatistics allows one to simulate an infinite number of different realizations (or observations). There is a need to capture the essence of that reservoir while also maintaining the integrity of the data, which geostatistics addresses.

3D geocellular models have previously been used to perform an accurate assessment and/or calculation of hydrocarbon plays, upon which sound development strategies and designs have been made (Kam et al., 2014; Saikia, Ikuku and Sarkar, 2017). This takes into account the risks and uncertainty assessments to which the stochastic nature (random probabilities) of 3D modelling lends itself (El Saadi, 2015).

The structure of a geocellular model is such that the 3D grid consists of a lattice whose values are defined by the user, to which various reservoir and/or petrophysical properties can be assigned. A simple grid should be used to facilitate the computation of dynamic simulations and to reduce the complexity of the model (Zakrevsky, 2011).

Schlumberger's Petrel ® software allows one to create a model and simulate production by taking into consideration the structural, petrophysical and stratigraphic properties of the reservoir. It extracts and integrates as much data as possible from various sources, giving connectivity within the reservoir. The properties used in the modelling, including rock and fluid properties i.e. porosity and permeability, are captured within these domains instead of being modelled as stand-alone.

Models are only as good as the data used to constrain them, and the decisions of the modeller. These should be decisions that are geologically sound and defendable within a reasonable limit. The use of one set of data thus subjects the model to a bias, and eliminates realistic geologic structure and heterogeneity. It is recommended that more than one dataset be used to reduce bias (El Saadi, 2015; Olson, n.d.), this includes structural, stratigraphic, and petrophysical data. A number of probable scenarios that take into account the various data are created by the user in order to honour the data and eliminate bias.

This study uses stratigraphic and petrophysical data, and has excluded structural data. The geologic structure of the model is thus subjected to bias. The bias will only have implications when running shale gas production forecasts, which is not in the scope of the study.

Spatial Variability: Variograms, Kriging and Simulation

While modelling petrophysical properties (porosity, permeability and saturation) in this study, comparison was made between Kriging and conditional simulation to choose the best one according to the variograms produced from the logs in the Petrel® software. Sequential Gaussian simulation was chosen to be the best representative for the porosity distribution.

Spatial variability and correlation in data sets plays quite a significant role in modelling as they add to the adequacy of the resulting data that is used. Generally, data values that are closer in space bear a high likelihood of similarity than data that are further apart. This is where the use of variograms comes in, to measure and describe the spatial correlation of the data sets such as porosity and permeability (Caers, 2005).

Variograms display variability between data points as a function of distance. Frequently the experimental variogram is used as a mode of analysis of the spatial covariance of a data set. The characteristics that are analysed in the variogram are known as *nugget*, *sill* and *range* **(Figure 2.2)** which are estimated by the fitting of a theoretical variogram model (Mälicke et al., 2018).

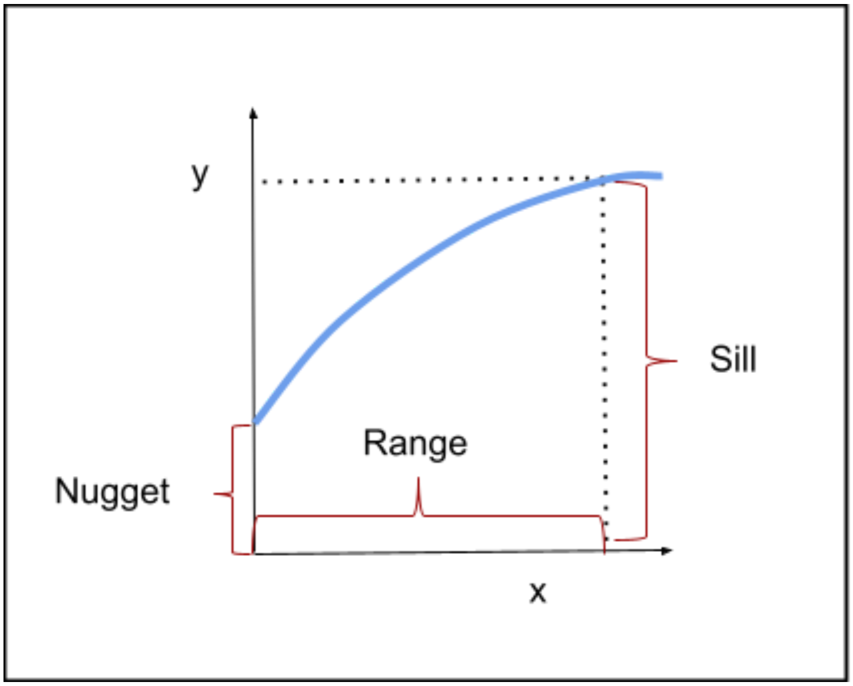

Figure 2.2. The morphology of a theoretical variogram, showing the nugget, sill, and range.

The variogram begins at the origin or sometimes at another value above the origin (termed nugget effect) and reaches a plateau. The origin of the variogram and its behaviour at that point is important and shows how the data varies spatially over short distances. This will show you whether change occurs rapidly at short distances or over large distances (El Saadi, 2015).

The *range* of the variogram is the distance from the origin to where it intersects the stationary point (along the x-axis) or flattens out, at which variability between data pairs is constant. This gives the average distance of correlation for a determined property in a specific direction. The value at which the stationary point is reached is the *sill*, which represents the overall statistical variance of the variable (this is the y-value corresponding to the *range*).

Types of variogram models

The most frequently used variogram models in geostatistics are (Caers, 2005; Mälicke et al., 2018) **(Figure 2.3)**:

- Spherical

  This is the most commonly used model. It is a low range variogram that assumes that correlations are equal to zero at all significant large distances.

- Exponential

  Describe correlation lengths over longer distances, where spatial autocorrelation decreases with increasing distance. Irregularly patterned data sets can be fitted better with this model. Unlike the spherical model, it assumes that correlations never vanish even at significantly large distances.

- Gaussian

  Normal probability distribution curves are used in this model. The model is used when you have continuous data sets, making it useful when you have attributes that are similar over short distances.

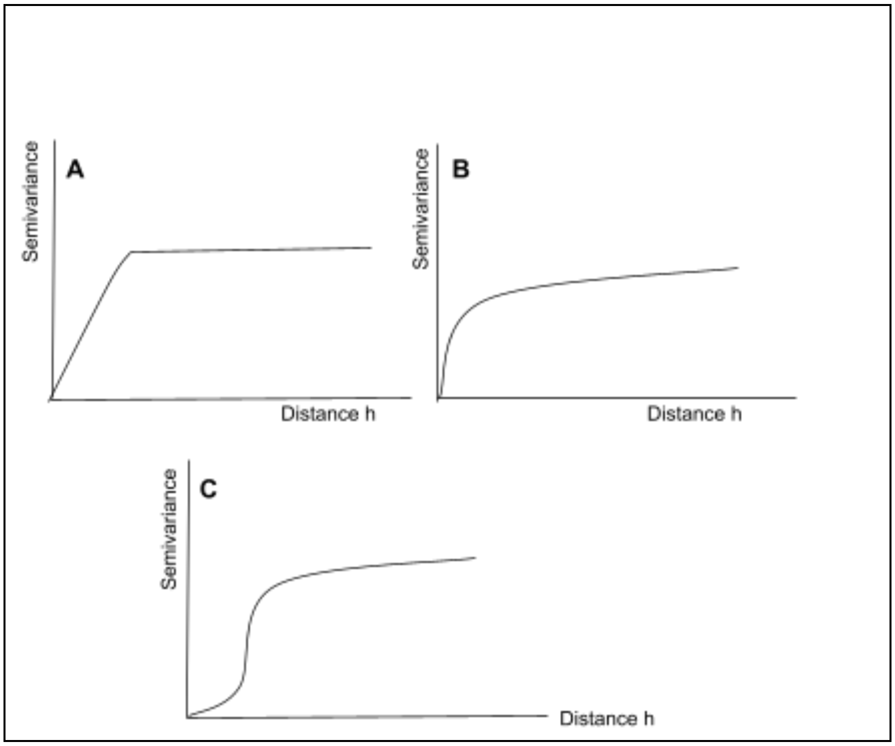

Figure 2.3. The three most frequently used theoretical variograms in geostatistics: spherical (A), exponential (B), and Gaussian (C).

Variograms are used as the main input in the process of Kriging. Kriging methods aim to limit the difference in the estimated value and the true value, and when expanded mathematically can be expressed as an order of linear equations that relate the variances for all points of data (Caers, 2005; El Saadi, 2015). The Kriging method tries to reduce the probable error that may result from a lack of geological reality and heterogeneity. It should however be used with caution especially in cases where the property in question shows high degrees of variability. The result may be too smooth or homogenous, which is experienced when only using Ordinary Kriging (which is a form of Kriging) to model (El Saadi, 2015).

Nugget Effect

The *nugget* is termed to be in effect when the variance does not go through the origin of the plot **(Figure 2.2)**. This indicates that the data show some variability even at very close distances, sometimes even at zero. This can be used to demonstrate the margin of error in the data or the apparent discontinuity at the origin which can be interpreted as the noise in the data (Caers, 2005; Camana and Deutsch, 2019; Chambers, Yarus and Hird, 2000). This is an indication of measurement errors which can be removed by applying the nugget to the variogram.

Kriging

Kriging is a gridding method which uses estimation to create a model from scattered data sets with z-values. The method is based on the assumptions that: (1) an unknown point value can be estimated from the values of neighbouring points even though the unknown point is not necessarily dependent on the other known values, and (2) variability in the z-values are a function of distance and direction, where less variability is observed in points that are close together than points further apart. With direction, points that lie along the same bearing will show less variability than points located along different bearings (Chambers, Yarus and Hird, 2000; Oliver and Webster, 1990). It is known to then bring out directional influences in your data, making it useful when there is directional bias in the data.

Ordinary Kriging

Ordinary kriging is the most commonly used method in geostatistics, first formally described by Matheron, G. It makes use of a known variogram to describe spatial variability at a point, by using known data from neighbouring points to the one being estimated (Kitanidis, 1997; Matheron, 1963; Wackernagel, 1995). The concern with ordinary kriging is whether it is reasonable to assume a constant mean across the field of data points. This makes it suitable to use with data that have an observed trend (Abdessattar, Dimitriy and Messaoud, 2019; Kumar Adhikary, Muttil and Gokhan Yilmaz, 2016).

Conditional Simulation

Conditional simulation is a popular method in the petroleum industry for the characterization of reservoirs with a degree of heterogeneity. While Kriging only captures spatial continuity, conditional simulation reflects both continuity and variability of the attributes by creating multiple realizations (Chambers, Yarus and Hird, 2000; Ersoy and Yünsel, 2006; Wackernagel, 2013). Statistics that are not related to the data linearly can then be computed. Gaussian conditional simulation is an approach that simulates realizations of a random Gaussian function with a known covariance function $C(h)$ (Shafer, 2006; Wackernagel, 2013). It provides a better representation of local heterogeneity that may be lost in Kriging, especially Ordinary Kriging.

Simulations are considered to be conditionally simulated if it has managed to honour the original data and reproduce the same spatial characteristics as the original data (Ersoy and Yünsel, 2006). This method is preferred as it can give more accurate results than methods of interpolation.

2.2.3 Integrated modelling approach

When creating a 3D geological model, geophysical and available geological data are incorporated in order to create a geocellular grid and structural framework of the reservoir. A distribution of lithofacies within the reservoir layers is then generated from well log data. Following this, reservoir petrophysical properties, which include porosity and permeability (assumed to be negligible in this study) are populated into the lithofacies model to create a spatial distribution model. Reservoir fluid flow principles are applied and solved numerically in order to create a dynamic model (simulation) of gas in place and technically recoverable gas (Mohaghegh et al., 2012; Saikia, Ikuku and Sarkar, 2017). This is described in these steps (Saikia, Ikuku and Sarkar, 2017):

Step 1: 3D Geocellular Modelling

There is a wide range of mathematical algorithms and methods that are used in creating 3D basin models, but only two common algorithms are used for the scope of this study. The algorithms are Sequential Gaussian Simulation (SGS) and Plurigaussian Simulation (PGS). SGS in comparison to the Kriging method, provides a more accurate 3D model which keeps the spatial variation in samples. PGS is applied where you have complex geological sequences rather than a simple sequence. This approach uses random fields to define lithological facies, and it allows the integration of a geological concept into a stochastic mathematical model while maintaining a manageable 3D grid (Mariethoz et al., 2009). Due to the simple nature of this studies' dataset, SGS was used.

Step 2: 3D Basin and Reservoir Modelling

Once a suitable algorithm is chosen, basin modelling commences. The purpose of basin modelling is to reconstruct the geologic history of the basin and to establish the petrophysical properties of the reservoir. By reconstructing the history of the basin through time, temperature, and burial conditions that affect source rock maturation and hydrocarbon potential can be better understood.

Step 3: Integration

Results of the geocellular and basin modelling are incorporated in this step, to create a dynamic model. Production data, where available, are then used to calibrate the model in such a way that it is as close to the actual reservoir as possible (Mohaghegh et al., 2012). A good history-matched model is one that takes into consideration sound geological interpretation and valid explanations for the model (Kam et al., 2014). In this study, existing literature reserve estimates are used as reference for history matching as no production of shale gas in the Karoo Basin has commenced (Chere et al., 2017; Cole, 2014; Decker and Marot, 2012; de Kock et al., 2017; Geel et al., 2015).

CHAPTER THREE

RESEARCH METHODOLOGY

INTRODUCTION

To complete this report, historic data that were collected by SOEKOR in the initial exploration process were used, and subsequent published data related to the study. The boreholes were chosen for this study because they were observed to have gas occurrence. These boreholes are now archived at the Council for Geoscience (CGS) core library in Donkerhoek, Pretoria.

3.1 LIMITATIONS TO THE STUDY

This study mainly used the historical SOEKOR data and does not provide new data related to the Karoo Basin. It only seeks to estimate the hydrocarbon potential of the basin based on the currently available data.

Until new data come to light, this study has used an area that is known to fall within the designated sweet spot, as well as an area representative of the dolerite intrusion relationships to provide conclusions that can then be extrapolated across the basin. It needs to be acknowledged, however, that this may not be sufficient enough to account for the actual thermal effect that the dolerites had on the gas.

3.2 DATA COLLECTION AND PREPARATION

The main data sets that were used in this study are presented below.

- Deep boreholes drilled by SOEKOR: Three boreholes, CR1/68, VR1/66, and SC3/67 were used in this study. A summary of the locations of the boreholes is presented in **Table 3.1.** Geophysical logs were provided by Petroleum Agency South Africa (PASA). These logs include gamma-ray, caliper, total gas, sonic and neutron-density logs**.**
- Borehole tops (Formations) information was gathered from data published by Rowsell and de Swardt (1976). The surfaces used in this study are **(Figure 3.1)**:
  > Top of the Ecca Group
  > Top of the Whitehill Formation
  > Top of the Dwyka Group
- Petrophysical data such as porosity was derived from literature (Rowsell and de Swardt, 1976).

The horizons were selected to constrain the model to places where hydrocarbon occurrence is most likely. The Top Dwyka helped limit the occurrence/end of the Ecca Group.

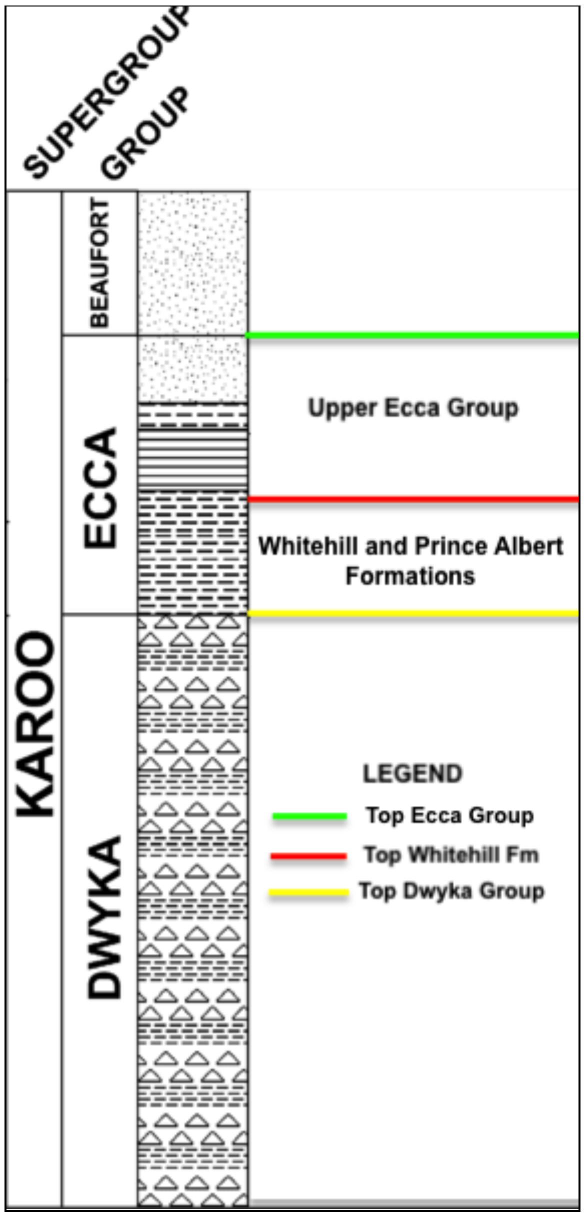

Figure 3.1 Stratigraphic log showing surfaces used in this study (modified after Herbert and Compton, 2007).

Table 3.1. Borehole localities and measured depth to top of the Ecca Group, Whitehill Formation, and Dwyka Group (depths from Rowsell and de Swardt, (1976)).

BOREHOLE	LAT/LONG Coordinates	UTM Coordinates	Measured Depth to top of Ecca Group (m)	Measured Depth to top of Whitehill Formation (m)	Measured Depth to top of Dwyka Group (m)
CR1/68	**Lat:** 32°29'9.24"S **Long:** 25° 0'28.08"E	**X:** 312895.8 **Y:** 6404006	2137	3671	3781
VR1/66	**Lat:** 32°13'29.28"S **Long:** 24°12'42.48"E	**X:** 237316.8 **Y:** 6431178	1300	2679	2778
SC3/67	**Lat:** 32°46'26.76"S **Long:** 24°17'54.60"E	**X:** 248955 **Y:** 6370511	2289	3972	4539

3.3 3D GEOLOGICAL MODELLING AND VOLUME ANALYSIS

3.3.1 Summary of Workflow

The below flowchart **(Figure 3.2)** gives a summary of the workflow that was used to complete this study.

- The relevant data were collected and prepared for input into Petrel®. This includes borehole data and borehole logs. Seismic interpretations were not used for this study as the horizons were already known from the physical core interpretations;
- Faults in the chosen study area were not modelled, so the building of the model began with the definition of a geocellular grid;
- A stratigraphic model was built based on the horizons (formation tops) and the zone definitions. This formed the framework into which all the other remaining properties and modelling was done;
- A facies model based on core-log defined facies was established;
- A porosity model was created and populated accordingly into the defined facies. Permeability was taken as negligible;
- Volumetric calculations were done for gas accumulations only, using gas saturations as the field is known to have only the occurrence of gas. These were compared with previous studies in other areas, and also with conventional methods of hydrocarbon volumetric calculations which are included in a later section;
- The workflow is presented in a linear fashion for the purpose of order, but in reality the modelling steps require repetitions before a final outcome can be decided upon.

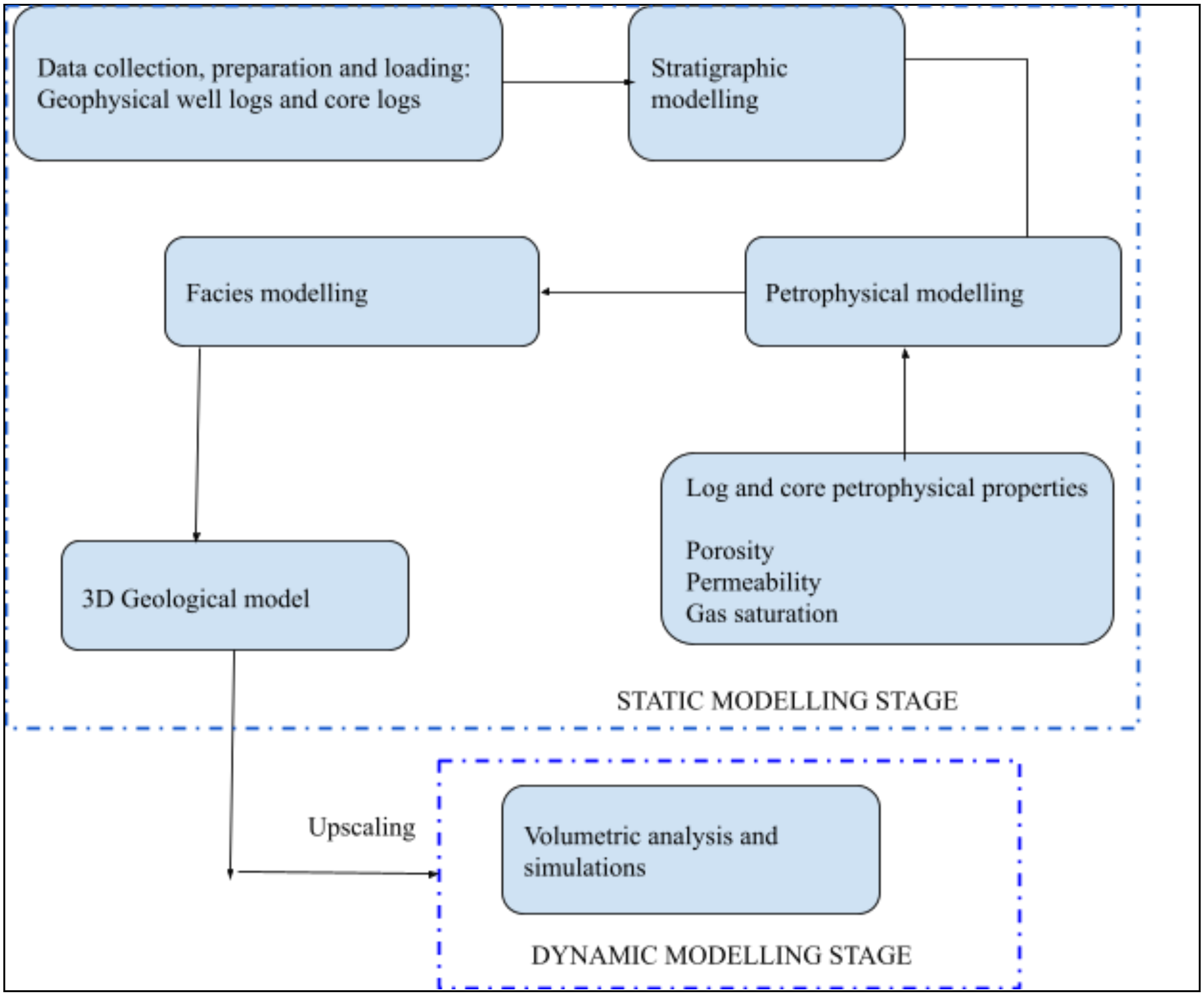

Figure 3.2. Summary of the workflow used in this study.

Detailed reports of the static and dynamic modelling stages is presented in the following segment **3.3.2**.

3.3.2 Modelling and Volumetric Analysis Workflow

Stratigraphic Modelling

The constraints of the model were the boreholes, formation tops, and facies determined from borehole log data and core data. This step is explained using the terminologies as they are in the Petrel® software.

Before modelling, the horizons and boundaries have to be defined to create a structural framework. In this particular case, it was the first step as no faults were included in the model for the study area. The boundaries of the model upon which the 3D framework was established was gridded using the Gaussian gridding method. For horizon modelling the Top Ecca Group - Top Whitehill Formation, Top Ecca Group - Top Dwyka Group, Top Ecca Group - Basement were modelled as conformable horizons, using well tops in order to honour borehole data. The thicknesses of the different formations making up the Lower Ecca Group are generally not differentiable using borehole logs alone, which is why the horizons were not split further beyond what is presented.

Once the horizons were established, they were divided into zones. The total of the zones was three, representative of the area between (1) Top Ecca Group to Top Whitehill Formation, (2) Whitehill and Prince Albert Formations, and (3) Top Dwyka Group, and Basement. The zones were then divided into layers using 'follow the top' method, to make computations easier **(Figure 3.3)**. The 'follow the top' method divides the horizons into layers following the horizon that is at the top of the zone, while remaining conformable to the base of the zone. Only the Top Ecca Group to Top Whitehill Formation, and Whitehill and Prince Albert Formations were layered, with 10 and 5 layers, respectively. The remaining zone was excluded because it lies beyond the area of interest.

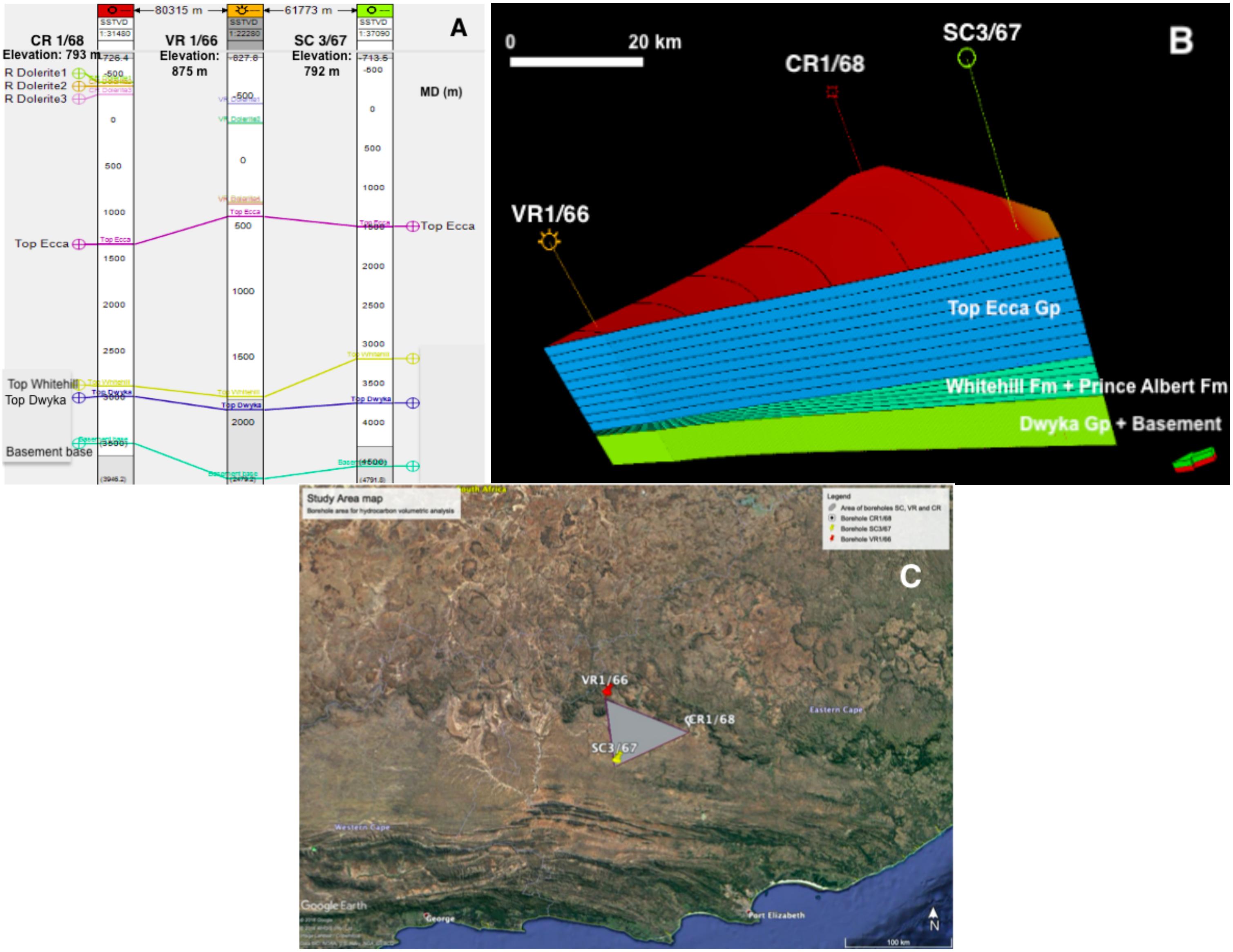

Figure 3.3. A: Horizons (formation tops) in the three boreholes according to the measured depth from borehole logs; B: The resulting zones and layering in 3D in Petrel® software; C: Location of boreholes on Google Earth map, and the area covered.

Petrophysical modelling

Porosity and total gas saturations were the petrophysical properties modelled. The 3D grid was populated with the values based on borehole data for porosity **(Table 3.2)**, and borehole logs for total gas saturations.

Table 3.2. Porosity values according to measured depth used in the modelling (from Rowsell and de Swardt, 1976).

CR 1/68	Measured Depth (m)	Porosity (%)	**VR 1/66**	Measured Depth (m)	Porosity (%)	**SC 3/67**	Measured Depth (m)	Porosity (%)
	3002	0.01		800	1		3852	0.4
	3500	0.01		950	1.22		3872	0.6
	3670	0.02		1156	1.34		3900	0.72
	3752	0.08		1203	1.46		3961	0.9
	3825	0.114		1548	1.5		4900	1.22
	3904	0.156		1623	1.88		5288	1.3
	4000	0.182		2100	1.97			
	4290	0.195		2200	1.99			
				2500	2.01			
				3300	2.3			

Log Upscaling

The process of upscaling logs averages the sample data from the processed logs that were put in the model. The original porosity and total gas logs are intrinsically fine scaled, while upscaling makes them coarser to enable quicker computing time. The porosity log and total gas logs were arithmetically averaged**.** Multiple upscaling iterations of the logs were computed, combining the individual logs until a suitable result representative of the original data and the study area was reached **(Figure 3.4a, Figure 3.4b)**.

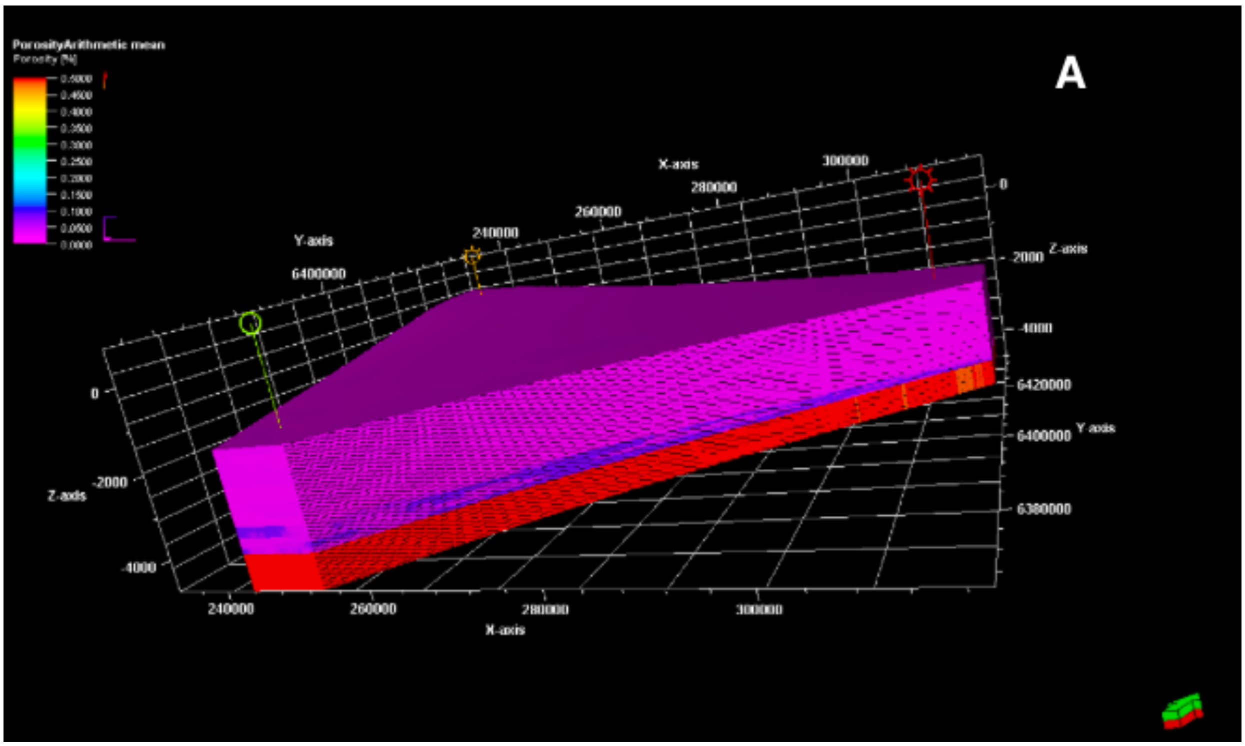

Figure 3.4A. 3D model showing upscaled porosity log. Colour indicators: purple indicates areas with porosity values of 0.0 - 0.05%, blue indicates areas with porosity values of 0.1%, and red indicates areas with porosity values of 0.5%.

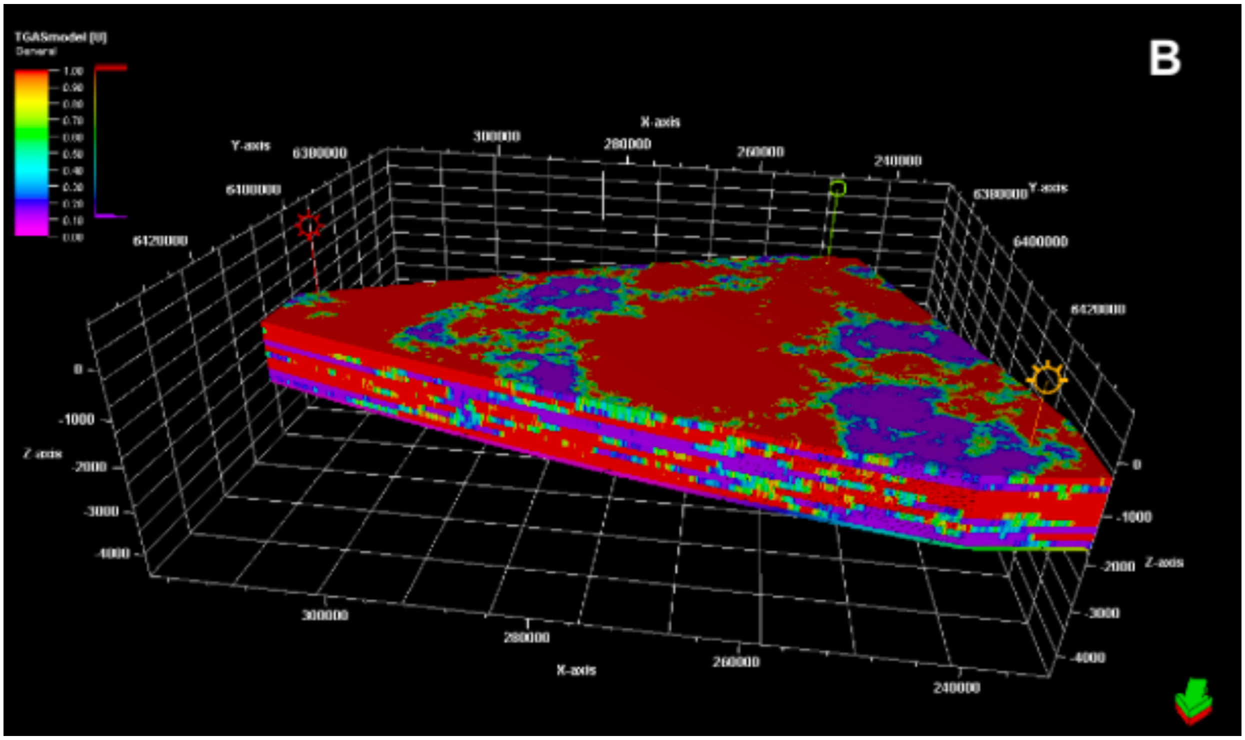

Figure 3.4B. 3D model showing upscaled total gas log. Colour indicators: purple indicates areas with gas saturation values of 0.0 - 0.1, blue indicates areas with gas saturation values of 0.2 - 0.4, green indicates areas with gas saturation values of 0.5 - 0.7, and red indicates areas with gas saturation values of 1.

Facies Modelling

The importance of a facies model is to preserve the geology of the 3D model. The facies were populated using the analysis of logs by Linol et al. (2016) **(Figure 3.5(A))**. They were then upscaled using the 'most of' averaging method, which selects the most representative data value for each cell in the model (**Figure 3.5(B)).**

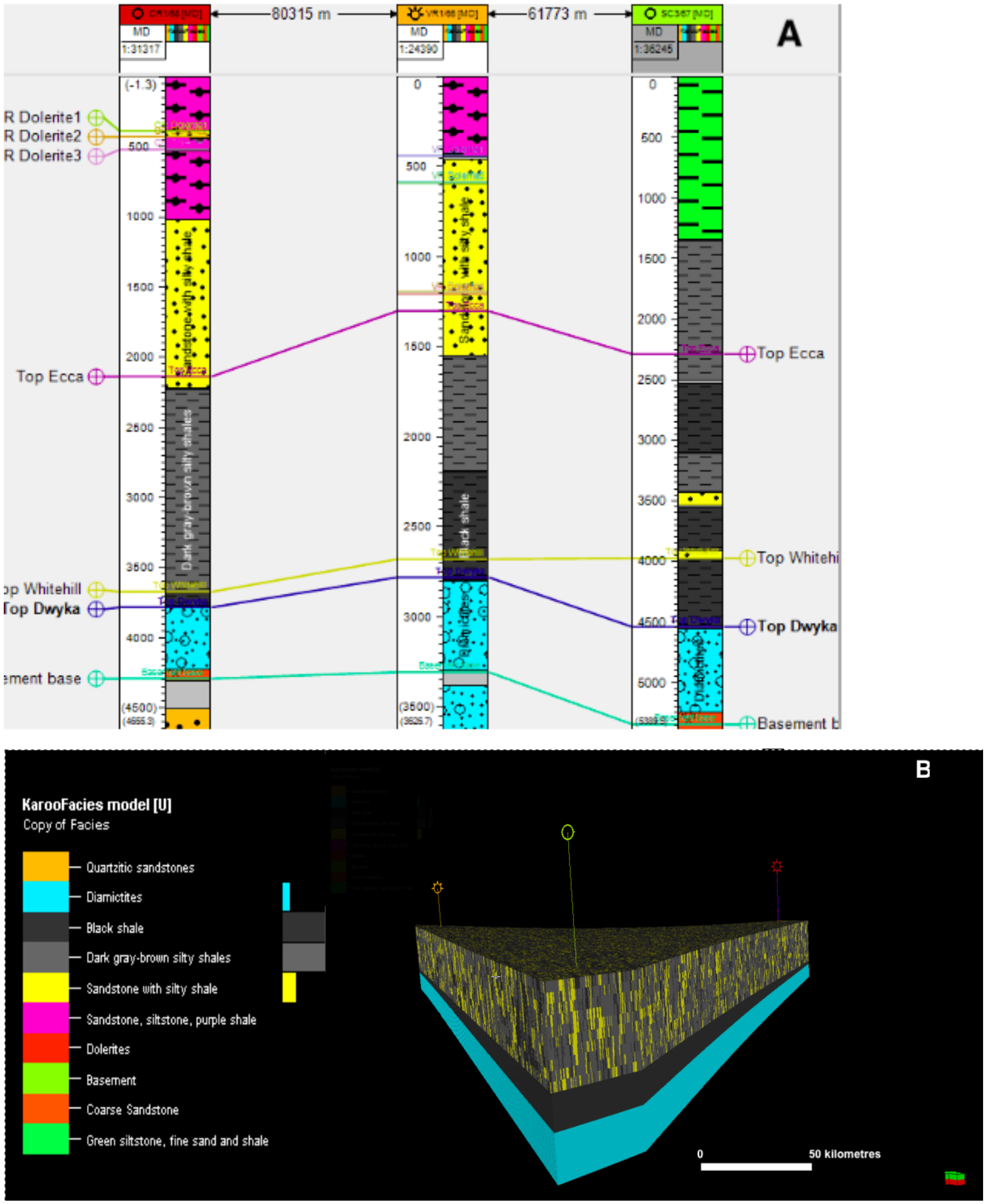

Figure 3.5. (A) Distributed facies from borehole data; (B) 3D model of the upscaled facies.

The research approach used for this study was to populate the established 3D model with stratigraphic and porosity data, which allowed for dynamic simulation (of which the results are discussed in the next chapter) to estimate shale gas amounts.

CHAPTER FOUR
RESULTS AND DISCUSSION

In this section, we simulate the gas initially in place for the Upper Ecca Group (top of Ecca Group to top of Whitehill Formation) and lower Ecca Group (Whitehill Formation and Prince Albert Formation), and the technically recoverable reserves. These results are then validated manually using an equation to calculate gas initially in place and technically recoverable reserves.

4.1 RESULTS

4.1.1 Simulation Results

This section outlines the gas initially in place and the technically recoverable reserves results acquired from Sequential Gaussian Simulation (SGS) that was applied to the 3D model using Petrel® software. The gas initially in place and the technically recoverable reserves were simulated for the upper Ecca and the lower Ecca Group.

The porosity values used are from Rowsell and de Swardt (1976), and were determined from historical borehole cores. The formation volume factor (Bg) values were sourced from calculations made by Chere et al. (2017) for boreholes CR1/68 and VR1/66. The third formation volume factor value used is an average from the two boreholes because borehole SC3/67 was not included in their study. Different probable scenarios (using different porosity, gas saturation and recovery factor) were then chosen using values representative of what is published for the Karoo Basin.

Table 4.1, Table 4.2, and Table 4.3 below summarize the reservoir parameters that wererespectively used in the simulation, the volumetric gas initially in place, and technically recoverable reserves results calculated for the individual horizons using recovery factors of 30, 75 and 90%. These recovery factors represent theoretical lowest, average and highest possibility of recovering the shale gas.

Table 4.1. Reservoir parameters used in simulation for the horizons top Ecca Group to top Whitehill Formation, and Whitehill and Prince Albert Formations, and the results of the gas initially in place estimates.

Horizon	**Scenario**	**1. Porosity (%)**	**2. Formation volume factor for gas at initial reservoir conditions**	**3. Gas saturation (Sg (1-Sw))**	**Gas initially in place (Tcf)**	**Average gas initially in place (Tcf)**
Top Ecca Gp to top Whitehill Fm	Scenario 1 Scenario 2 Scenario 3	0.095 0.856 1.667	0.00496 0.00705 0.006005*	0.1 0.5 0.9	3.03 96.08 395.4	164.8
Whitehill and Prince Albert Fms	Scenario 1 Scenario 2 Scenario 3	0.095 0.856 1.667	0.00378 0.00453 0.004155*	0.4 0.75 0.9	3.22 45.36 115.56	54.7

1 *from logs and core (Rowsell and de Swardt, 1976);* ***2*** *calculated by Chere et al., (2017);* ***3*** *from probable scenarios (Sg = 1-Sw).*

*****values are an average of the two values above it.*

Table 4.2. Results from simulation for the technically recoverable reserves estimates for top Ecca Group to top Whitehill Formation using variable gas saturations and recovery factor.

SCENARIO	**RF = 30%**	**RF = 75%**	**RF = 90%**
Scenario 1 **Porosity = 0.095** **Bg = 0.00496** **Sg = 0.1**	0.9 Tcf	2.3 Tcf	2.7 Tcf
Scenario 2 **Porosity = 0.856** **Bg = 0.00705** **Sg = 0.5**	28.8 Tcf	72.1 Tcf	86.5 Tcf
Scenario 3 **Porosity = 1.667** **Bg = 0.006005** **Sg = 0.9**	118.6 Tcf	296.6 Tcf	355.9 Tcf

Table 4.3. Results from simulation for the technically recoverable reserves estimates for Whitehill and Prince Albert Formations using variable gas saturations and recovery factor.

SCENARIO	**RF = 30%**	**RF = 75%**	**RF = 90%**
Scenario 1 **Porosity = 0.095** **Bg = 0.00378** **Sg = 0.4**	0.9 Tcf	2.4 Tcf	2.9 Tcf
Scenario 2 **Porosity = 0.856** **Bg = 0.00453** **Sg = 0.75**	13.6 Tcf	34.0 Tcf	40.8 Tcf
Scenario 3 **Porosity = 1.667** **Bg = 0.004155** **Sg = 0.9**	34.7 Tcf	86.7 Tcf	104.0 Tcf

4.1.2 Validation of Results

Gas Initially In Place Estimates

The results of the simulation were validated by using the American Association of Petroleum Geologists (AAPG) volumetric calculation formula:

$$G = \frac{43560\ A \times h \times \phi\ (1 - Sw)}{Bg}$$

where:

- G is Original Gas In Place (OGIP)
- 43560 is the conversion factor from acre-feet to feet^3
- A is the area of the reservoir measured from map, in acres. The area covered by the boreholes was acquired from Google Earth **(Figure 3.3)**.
- h is the height or thickness of pay zone from borehole data in feet
- ф is porosity from log and core data
- 1-Sw is the gas saturation from reference data
- Bg is the formation volume factor for gas at initial reservoir conditions

This was applied to the two horizons of interest, Top Ecca Group to Top Whitehill Formation, and Whitehill and Prince Albert Formations.

Table 4.4 below summarizes the reservoir parameters and calculated gas initially in place that were used in the validation of the simulation results.

Table 4.4. Reservoir parameters used in the calculation of gas initially in place for the horizons top Ecca Group to top Whitehill Formation, and Whitehill and Prince Albert Formations.

Horizon	Area (acres)	Thickness of zone (m)	Porosity (%)	Formation volume factor	Gas saturation	Gas initially in place (Tcf)	Average gas initially in place (Tcf)
Top Ecca to top Whitehill	526 042	1532.0*	0.095 0.856 1.667	0.00496 0.00705 0.006005	0.1 0.5 0.9	2.21 69.92 287.8	119.9
Whitehill and Prince Albert Formations	526 042	258.66*	0.095 0.856 1.667	0.00378 0.00453 0.004155	0.4 0.75 0.9	1.95 27.49 70.05	33.2

calculated average thickness across the three boreholes (CR1/68, VR1/66 and SC3/67), from borehole depths in Table 3.1.

Technically Recoverable Reserves Estimates

From the values of the GIIP in **Table 4.4**, TRR estimates were validated using AAPG formula:

$$Recoverable\ Gas = GIIP \times RF$$

where:

RF is the probable recovery factor using the lowest estimate (30%) to the highest recovery of gas (90%).

Table 4.5 and **Table 4.6** below give a summary of the results of the technically recoverable reserve arising from the validation of the simulated results with unchanged reservoir parameters.

Table 4.5. Technically recoverable reserves estimates for top Ecca Group to top Whitehill Formation using gas initially in place determined from AAPG formula and variable gas saturations and recovery factors.

SCENARIO	**RF = 30%**	**RF = 75%**	**RF = 90%**
Scenario 1 **Porosity = 0.095** **Bg = 0.00496** **Sg = 0.1**	0.7 Tcf	1.7 Tcf	2.0 Tcf
Scenario 2 **Porosity = 0.856** **Bg = 0.00705** **Sg = 0.5**	20.9 Tcf	52.4 Tcf	62.9 Tcf
Scenario 3 **Porosity = 1.667** **Bg = 0.006005** **Sg = 0.9**	86.3 Tcf	215.9 Tcf	259.0 Tcf

Table 4.6. Technically recoverable reserves estimates for Whitehill and Prince Albert Formations using gas initially in place determined from AAPG formula and variable gas saturations and recovery factors.

SCENARIO	**RF = 30%**	**RF = 75%**	**RF = 90%**
Scenario 1 **Porosity = 0.095** **Bg = 0.00378** **Sg = 0.4**	0.6 Tcf	1.5 Tcf	1.8 Tcf
Scenario 2 **Porosity = 0.856** **Bg = 0.00453** **Sg = 0.75**	8.2 Tcf	20.6 Tcf	24.7 Tcf
Scenario 3 **Porosity = 1.667** **Bg = 0.004155** **Sg = 0.9**	21.0 Tcf	52.5 Tcf	63.0 Tcf

4.1.3 Comparison of Results

In this section, the simulated and calculated results are visually compared to analyse the margin of error. The simulated versus calculated gas initially in place, and technically recoverable reserves results for top Ecca Group to the top Whitehill Formation are presented in **Figure 4.1**. The simulated versus calculated gas initially in place, and technically recoverable reserves results for the Whitehill and Prince Albert Formations are presented in **Figure 4.2**.

In **Figure 4.1** (Top Ecca Group to top Whitehill Formation) the simulation results are 27% higher than the calculated results for the 3 scenarios, for the gas initially in place and effectively, the technically recoverable reserves. In **Figure 4.2** (Whitehill and Prince Albert Formations) the simulation results are 39% higher than the calculated results for all 3 scenarios, for gas initially in place and effectively, the technically recoverable reserves This may be because the model takes into account other factors that the formula does not, including lithological data. The greatest difference, being 39% between the simulated and calculated values is observed in the Whitehill and Prince Albert Formations than in the top Ecca Group to the top Whitehill Formation. The amount of recoverable gas is directly proportional to the recovery factor. This can be seen in the technically recoverable reserves graphs where the estimates are lowest at 30% and highest at 90% recovery factor. Increasing gas saturation and porosity are expected to play a role in higher proportions of extracted/estimated gas and this is true in this study too (see **Appendix 2**).

Top Ecca Group to top Whitehill Formation

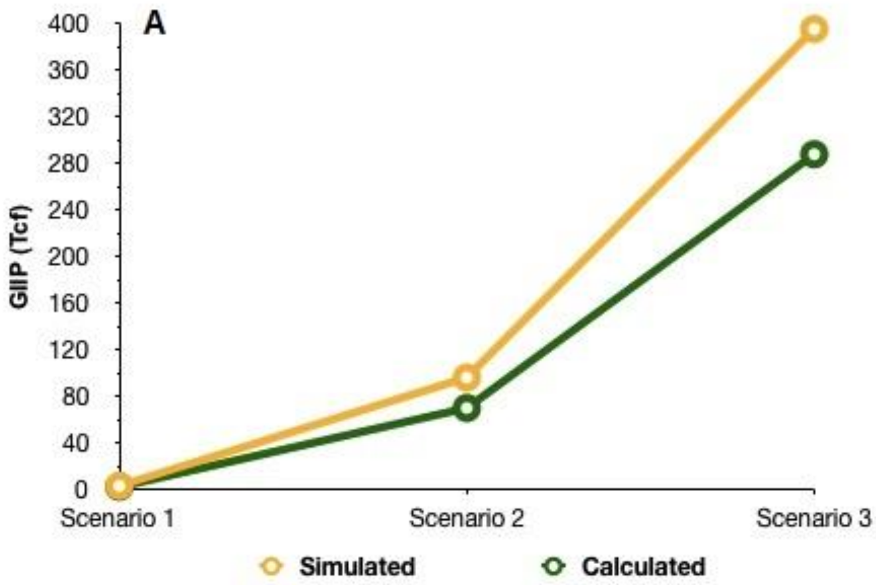

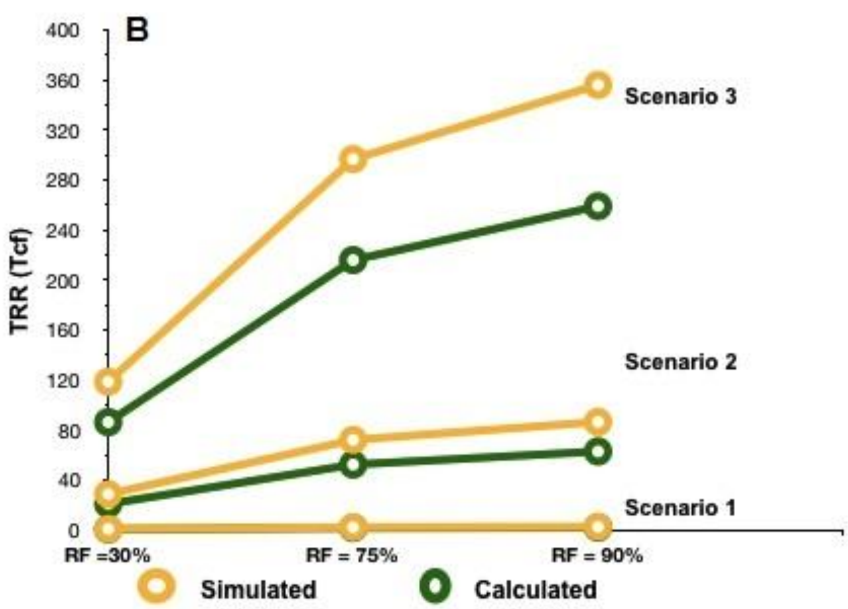

Figure 4.1. A: Simulated vs. calculated gas initially in place and; B: Simulated vs. calculated technically recoverable reserves results for the top Ecca Group to top Whitehill Formation. GIIP is gas originally in place, TRR is technically recoverable reserves, and RF is the recovery factor.

Whitehill and Prince Albert Formations

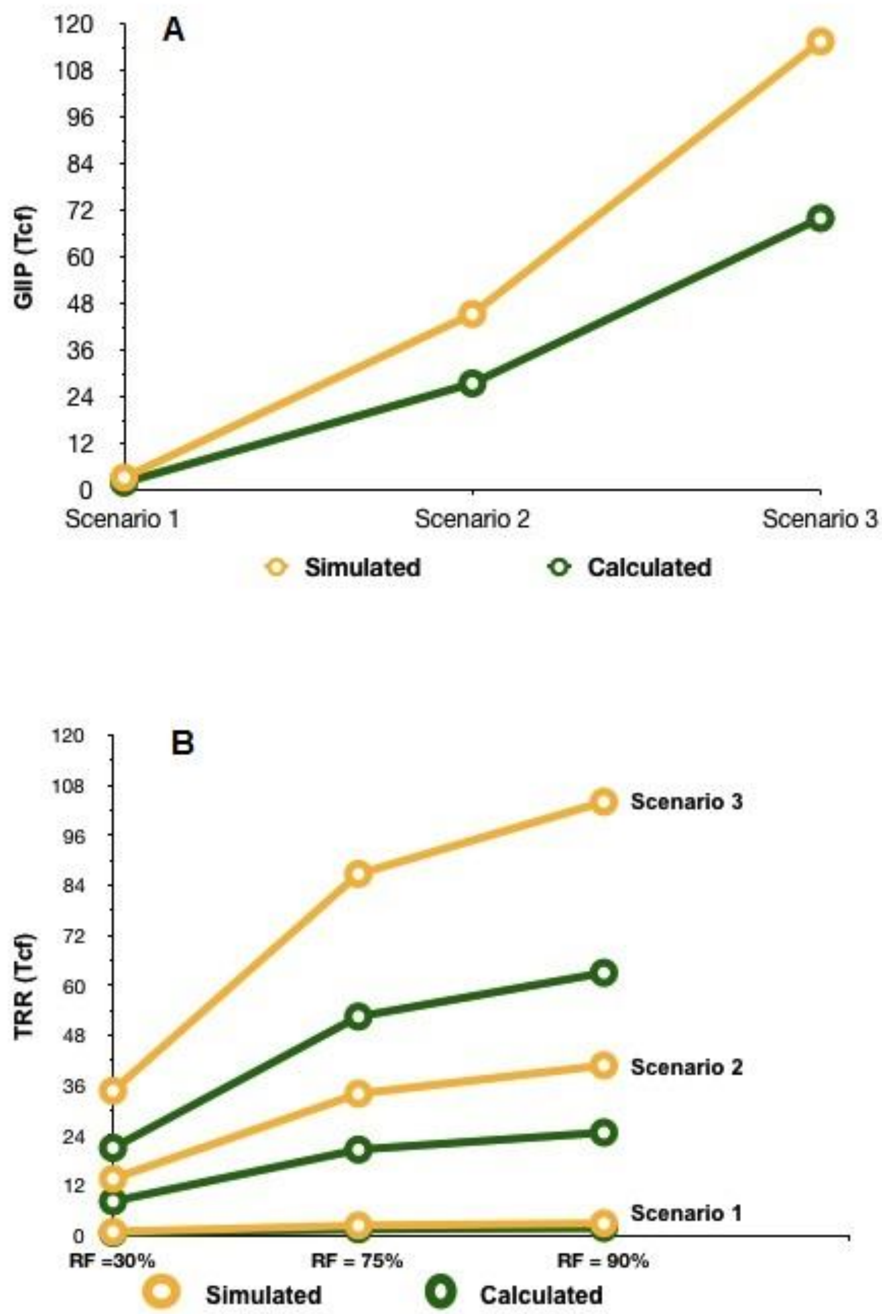

Figure 4.2. A: Simulated vs. calculated gas initially in place and; B: Simulated vs. calculated technically recoverable reserves results for the Whitehill and Prince Albert Formations. GIIP is gas originally in place, TRR is technically recoverable reserves, and RF is the recovery factor.

Averaged simulated and calculated results

The final estimates are an average of the simulated and calculated results, at recovery factors of 30, 75 and 90% as seen in **Figure 4.3**.

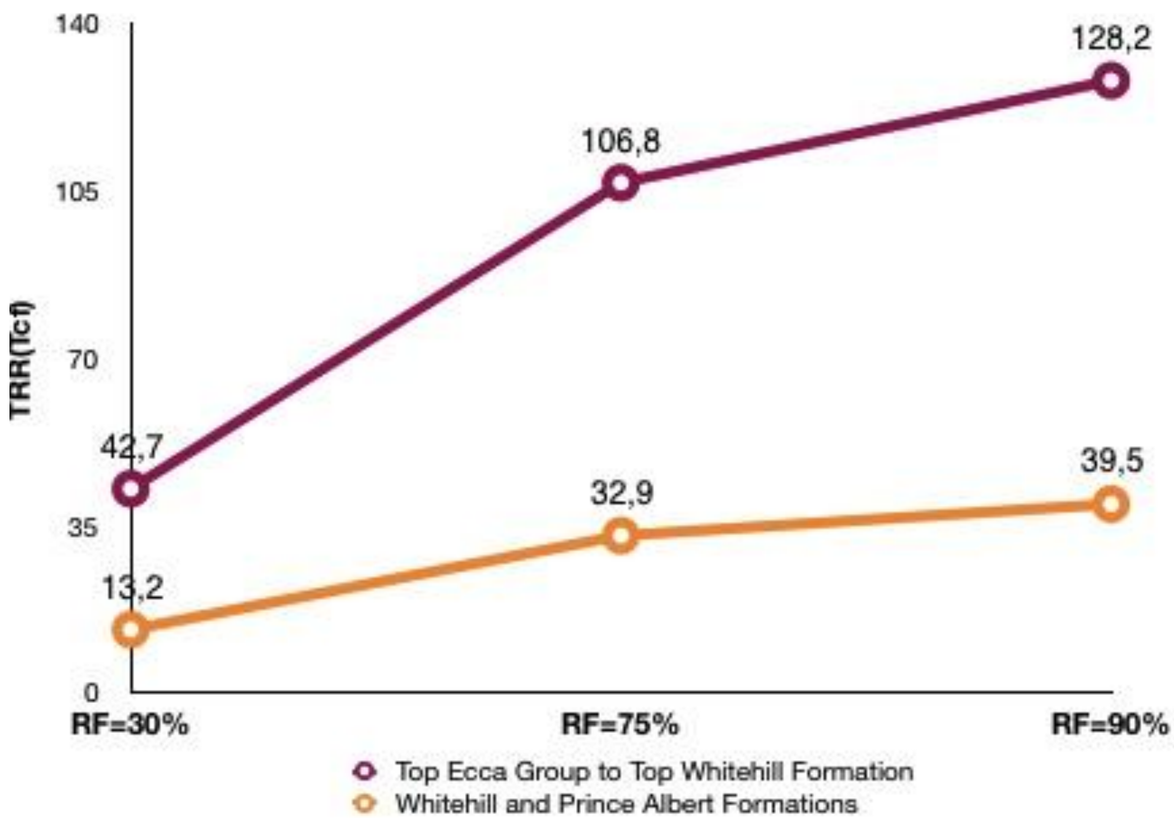

Figure 4.3. The averaged simulated and calculated technically recoverable reserves results for the top Ecca Group to top Whitehill Formation, and Whitehill and Prince Albert Formations. TRR is technically recoverable reserves, and RF is the recovery factor.

Comparison with existing literature results

In this section, the results of this current study are compared with previously published reports for the assessment of the potential of the Karoo Basin. These studies used different assessment methods from this study. It should be noted that the simulation method used in this study has never been applied to the Karoo Basin but has been used in other basins, even the Bredasdorp which is off the southern coast of South Africa (El Saadi, 2015).

As shown in **Figure 4.4** and **Figure 4.5**, the average TRR results assuming a recovery factor of 30% for the Upper Ecca match the results of Chere et al. (2017). At higher recovery factors (75 and 90%), the results for the Upper Ecca do not match. The results for the Whitehill and Prince Albert Formations also match those from Chere et al., (2017), Geel et al., (2015), and de Kock et al., (2017). However, as shown in **Figure 4.6**, the averaged values for the Whitehill and Prince Albert Formations do not fit the results of Decker and Marot (2012), and Cole (2014). This could be due to the variable 'sweet spot', as well as to the methods of investigation applied.

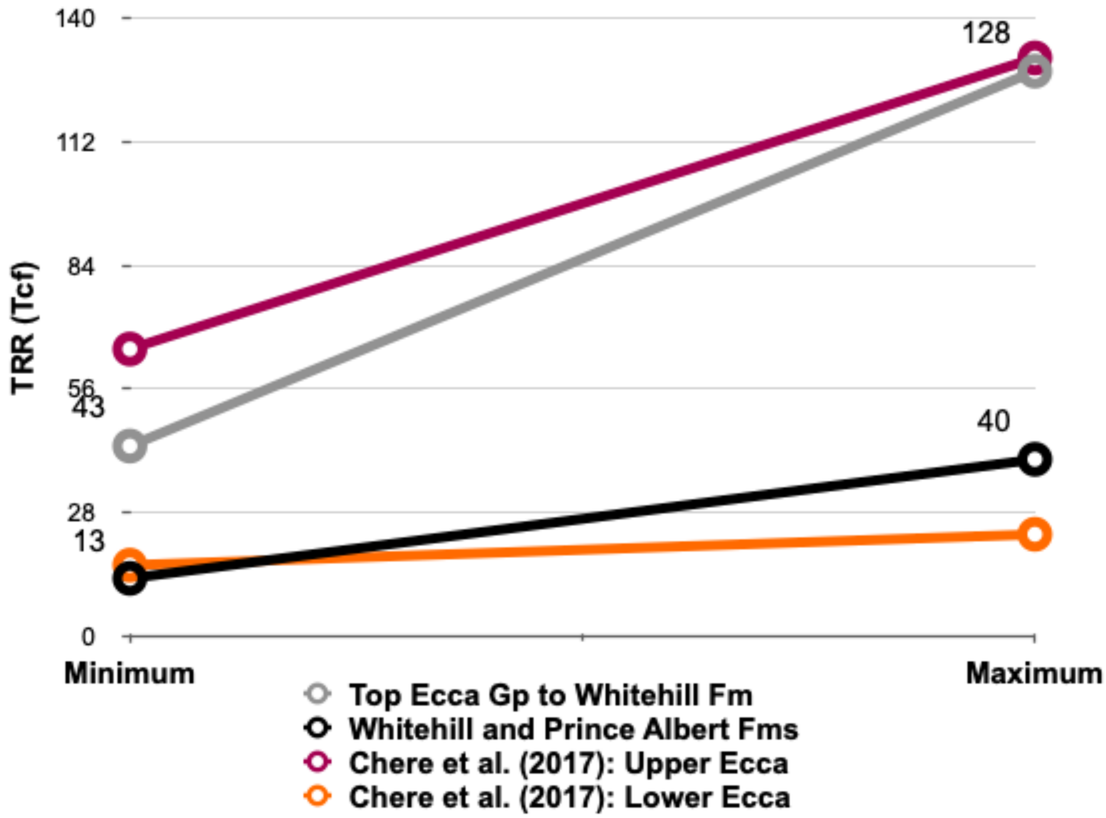

Figure 4.4. Comparison of averaged technically recoverable reserves (TRR) results with those from Chere et al. (2017) for the Upper and Lower Ecca Group.

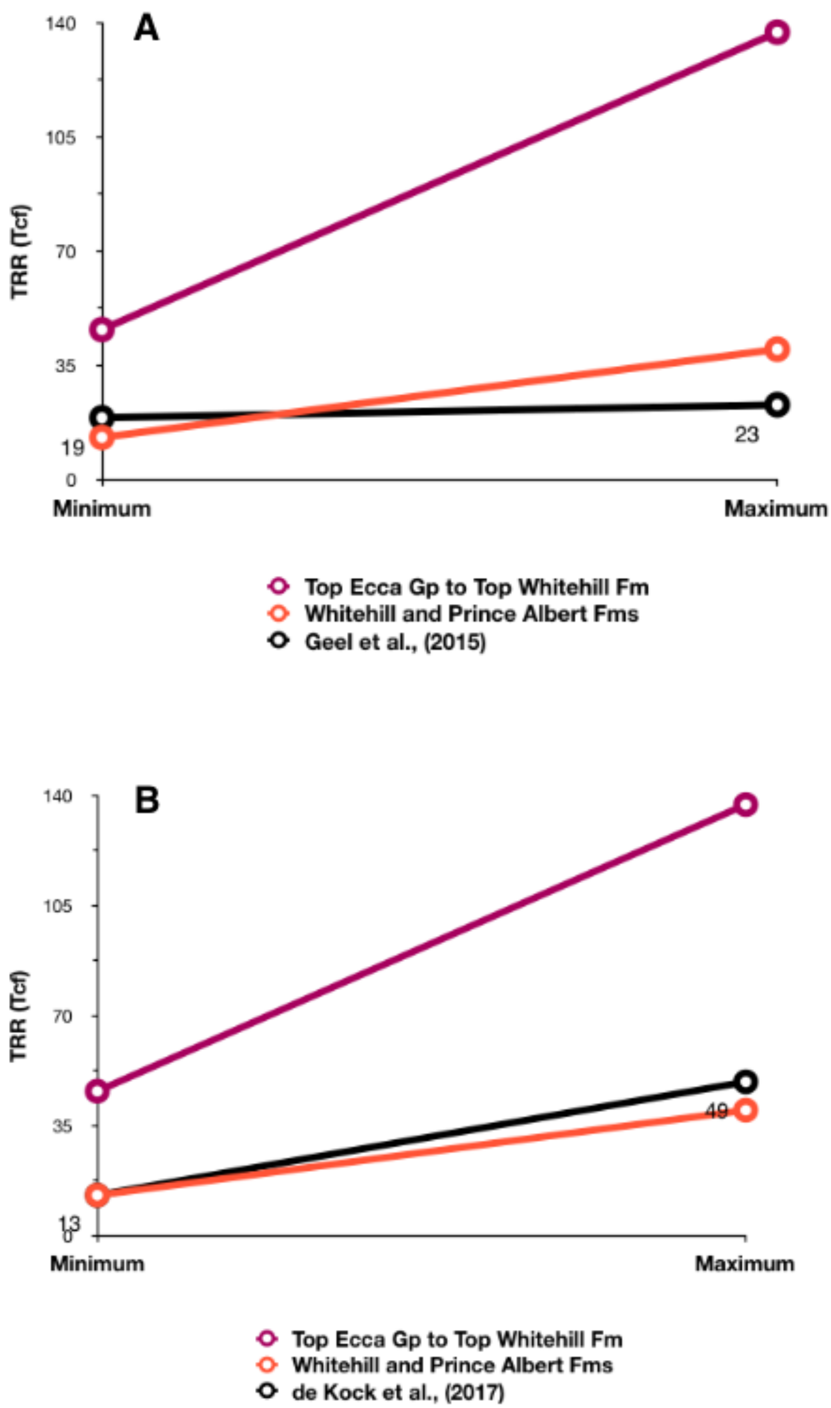

Figure 4.5. Comparison of averaged technically recoverable reserves (TRR) results with those from (A) Geel et al. (2015) and (B) de Kock et al. (2017) for the Lower Ecca Group.

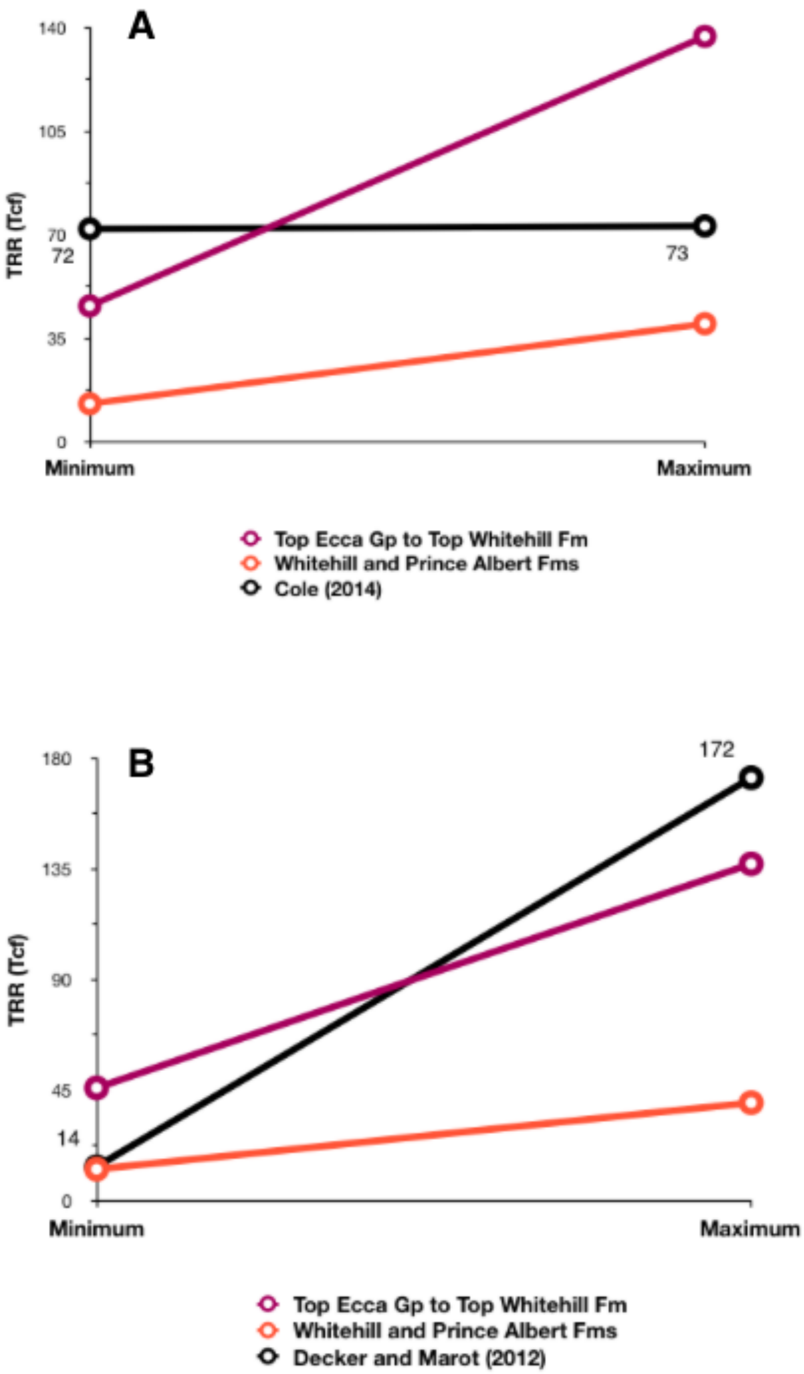

Figure 4.6. Comparison of averaged technically recoverable reserves (TRR) results with those from (A) Cole (2014), and (B) Decker and Marot (2012) for the Lower Ecca Group.

4.2 SUMMARY OF DISCUSSION

This report is a local assessment study of the Upper Ecca (Top Ecca to top Whitehill Formation) and Lower Ecca (Whitehill and Prince Albert Formations) in the southeastern Karoo. All the results are based on the methodologies described in Chapter 3 and 4.

The objectives of this study were to establish a geological model and to run simulations using Petrel® software. Based on this model, the effect of changing reservoir parameters (i.e porosity and gas saturation) was studied. Furthermore, assuming recovery factors of 30, 75 and 90%, we estimated the gas initially in place (GIIP) and technically recoverable reserves (TRR). These results were validated by the previous results of Chere et al. (2017), Geel et al. (2015), and de Kock et al. (2017). The limitations of our results are that they do not take into consideration the quantified localised thermal effect that the dolerites might have had on the gas. Studies have shown that there is a possible effect that the dolerites have had but this has also not been quantified (Chere et al., 2017; de Kock et al., 2017; Geel et al., 2015). We however feel that a recovery factor of 30% is reasonable given the economic implications the dolerites could pose on the extraction of the gas, and the environmental precautions surrounding the production of shale gas in the Karoo Basin.

CHAPTER FIVE

CONCLUSIONS AND RECOMMENDATIONS

5.1 CONCLUSIONS

The 3D Geocellular Modelling workflow was used to estimate hydrocarbon volumetrics with changing parameters and taking into consideration other factors such as facies changes. The objectives of this research were fulfilled and thus the technically recoverable reserves (TRR) estimates of this study are 43 Tcf - 128 Tcf (with an average of 107 Tcf) for the Upper Ecca Group (top Ecca Group to top Whitehill Formation), and 13 Tcf - 40 Tcf (with an average of 33 Tcf) for Whitehill and Prince Albert Formations. These estimates take into consideration the variable recovery factors (30, 75 and 90%) for production.

When comparing the results of this study with previous studies, the estimates can be considered to fall within the ranges of those studies. The results are most consistent with the work of Geel et al., (2015), Chere et al., (2017) and de Kock et al., (2017). All these estimates indicate that the Karoo Basin is an economic target of shale gas.

It is not recommended that the estimates of this study be extrapolated across the whole basin as there is no supporting data to show that the study area is representative of the basin. Accordingly, this study can be regarded as a basis for future improvements and enrichment of the modelling workflow.

5.2 RECOMMENDATIONS

The sparseness of data in the basin makes it difficult to conduct reliable analyses and conclusions. A significant improvement of the estimates can be observed if uncertainty is reduced, by re-examining the data currently available in order to obtain better constraints on depth, thickness, total organic content (TOC), porosity, maturity, gas saturation, and reservoir temperature and pressure of shale formations such as Chere et al., (2017). New data is also needed, i.e deep boreholes, and seismic surveys, so that further analyses and estimates can be done with more confidence. The information will help increase the success of the play and also decrease the range of uncertainty in the estimates. The newly gathered information could easily be run through the workflow/methodology used in this study to update the estimates of gas initially in place (GIIP) and technically recoverable reserves (TRR).

REFERENCES

Aarnes, I., Podladchikov, Y. and Neumann, E. (2008). Post-emplacement melt flow induced by thermal stresses: Implications for differentiation in sills. *Earth and Planetary Science Letters*, [online] 276(1-2), p.153.

Abdessattar, L., Dimitriy, N. and Messaoud, M. (2019). Geostatistical Modeling by the Ordinary Kriging in the Estimation of Mineral Resources on the Kieselguhr Mine, Algeria. In: *IOP Conference Series: Earth and Environmental Science*.

Academy of Science of South Africa (2016). *South Africa's Technical Readiness to Support the Shale Gas Industry*. [online] Pretoria: Academy of Science of South Africa (ASSAf), pp.23-25.

Aplin, A. (2000). Seals, Traps and the Petroleum System. *Marine and Petroleum Geology*, 17(9), p.1083.

Baiyegunhi, C., Nxantsiya, Z., Pharoe, K., Baiyegunhi, T. and Mepaiyeda, S. (2019). Petrographical and geophysical investigation of the Ecca Group between Fort Beaufort and Grahamstown, in the Eastern Cape Province, South Africa. *Open Geosciences*, 11(1), pp.313-326.

Camana, F. and Deutsch, C. (2019). *The Nugget Effect*, pp.1-5.

Chambers, R., Yarus, J. and Hird, K. (2000). Petroleum geostatistics for nongeostatisticians. *The Leading Edge*, 19(5), pp.474-479.

Chere, N., Linol, B., de Wit, M. and Schulz, H. (2017). Lateral and temporal variations of black shales across the southern Karoo Basin - Implications for shale gas exploration. *South African Journal of Geology*, 120(4), pp.541-564.

Cole D. Geology of Karoo shale gas and how this can influence economic gas recovery. Gas - The game changer for South Africa?! Paper presented at: Fossil Fuel Foundation Conference; 2014 May 12; Johannesburg, South Africa.

Costin, G., Götz, A. and Ruckwied, K. (2019). Sedimentary organic matter characterization of the Whitehill shales (Karoo Basin, South Africa): An integrated quantitative approach using FE-EPMA and LA-ICP-MS. *Review of Palaeobotany and Palynology*, [online] 268, p.31.

Council for Geoscience (2016). *Shale gas in the Karoo*.

CSIR (2016). *Shale Gas Development in the Central Karoo: A Scientific Assessment of the Opportunities and Risks*. [online] Pretoria: CSIR.

de Kock, Michiel and Beukes, Nicolas and Götz, Annette and Cole, D. & Robey, Kate and Birch, A. and Withers, A. and Niekerk, H.S.. (2016). Open file progress report on exploration of the southern Karoo Basin through CIMERA-KARIN borehole KZF-1 in the Tankwa Karoo, Witzenberg (Ceres) district, pp.1-12.

de Kock, M., Beukes, N., Adeniyi, E., Cole, D., Götz, A., Geel, C. and Ossa, F. (2017). Deflating the shale gas potential of South Africa's Main Karoo basin. *South African Journal of Science*, 113 (9/10).

Dubrule, O. (1998). *Geostatistics in petroleum geology*. American Association of Petroleum Geologists, pp.1-100.

El Saadi, O. (2015). *A Geo-Cellular Model of a Multiphase Hydrocarbon Field incorporating Fault-Seal Analysis: Bredasdorp Basin, South Africa*. MSc. University of Cape Town.

Ersoy, A. and Yünsel, T. (2006). Geostatistical Conditional Simulation for the Assessment of the Quality Characteristics of Cayırhan Lignite Deposits. *Energy Exploration & Exploitation*, 24(6), pp.391-416.

Geel, C. (2013). *Geochemistry and petrophysics Lower Ecca Group, from core of a new bore hole north of Wolwefontein, Eastern Cape*. MSc. Nelson Mandela Metropolitan University.

Geel, C., De Wit, M., Booth, P., Schulz, H. and Horsfield, B. (2015). Palaeo-environment, diagenesis and characteristics of Permian black shales in the lower Karoo Supergroup flanking the Cape Fold Belt near Jansenville, Eastern Cape, South Africa: Implications for the shale gas potential of the Karoo Basin. *South African Journal of Geology*, [online] 118(3), pp.249-274.

Geel, C., Schulz, H., Booth, P., deWit, M. and Horsfield, B. (2013). Shale Gas Characteristics of Permian Black Shales in South Africa: Results from Recent Drilling in the Ecca Group (Eastern Cape). *Energy Procedia*, 40, pp.260-263.

Help.rockware.com. (n.d.). *What is a Variogram?*. [online] Available at: https://help.rockware.com/rockworks17/WebHelp/gridding_krig_variogram.htm.

Herbert, C. and Compton, J. (2007). Depositional environments of the lower Permian Dwyka diamictite and Prince Albert shale inferred from the geochemistry of early diagenetic concretions, southwest Karoo Basin, South Africa. *Sedimentary Geology*, 194(3-4), p.265.

Hongjun, W., Feng, M., Xiaoguang, T., Zuodong, L., Xinshun, Z., Zhenzhen, W., Denghua, L., Bo, W., Yinfu, X. and Liuyan, Y. (2016). Assessment of global unconventional oil and gas resources. *PETROLEUM EXPLORATION AND DEVELOPMENT*, [online] 43(6), pp.925-940.

Jarvie, D., Hill, R., Ruble, T. and Pollastro, R. (2007). Unconventional shale-gas systems: The Mississippian Barnett Shale of north-central Texas as one model for thermogenic shale-gas assessment. *AAPG Bulletin*, 91(4), pp.475-499.

Jarvie, D.M. (2012). Shale resource systems for oil and gas: Part 2 – Shale-oil resource systems. In: J.A. Breyer (Editor). Shale reservoirs – Giant resources for the 21st century: American Association of Petroleum Geologists Memoir, 97, pp. 89-119.

Johnson, M., Van Vuuren, C., Hegenberger, W., Key, R. and Show, U., 1996. Stratigraphy of the Karoo Supergroup in southern Africa: an overview. *Journal of*

African Earth Sciences, 23(1), pp.3-15.

Jonk, R., Allen, J., Magennis, L., Potma, K. and Wamsteeker, M. (2013). Constructing Meaningful Geologic Models of Shale Gas Systems: An Example from the Horn River Basin, Canada. *Unconventional Resources Technology Conference, Denver, Colorado, 12-14 August 2013*.

Kam, P., Omatsone, E., Kumar, A., Nadeem, M. and Novlesky, A. (2014). Integrated Geoscience and Reservoir Simulation Approach to Understanding Fluid Flow in Multi-Well Pad Shale Gas Reservoirs. In: *SPE/CSUR Unconventional Resources Conference.* Calgary, pp.5-9.

Kitanidis, P. (1997). *Introduction to Geostatistics: Applications to Hydrogeology*. Cambridge: Cambridge Univ. Press, pp.10-20.

Kumar Adhikary, S., Muttil, N. and Gokhan Yilmaz, A. (2016). Ordinary kriging and genetic programming for spatial estimation of rainfall in the Middle Yarra River catchment, Australia. *Hydrology Research*, 47(6), pp.1182-1197.

Kuuskraa V Stevens S, Van Leeuwen T, Moodhe K. World shale gas and shale oil resource assessment. Technically recoverable shale oil and shale gas resources: An assessment of 137 shale formations in 41 countries outside the United States. Washington DC: US Department of Energy; 2013. http://www.eia.gov/analysis/studies/worldshalegas/pdf/fullreport.pdf.

Labed, I., Oyeneyin, B. and Oluyemi, G. (2018). Gas-condensate flow modelling for shale reservoirs. *Journal of Natural Gas Science and Engineering*, 59, pp.156-167.

Lijun, L., Jun, Y., Hai, S., Zhaoqin, H., Xia, Y. and Longlong, L. (2019). Compositional modeling of shale condensate gas flow with multiple transport mechanisms. *Journal of Petroleum Science and Engineering*, 172, pp.1186-1201.

Linol, B., Chere, N., Muedi, T., Nengovhela, V, and Wit, M. (2016). Deep Borehole Lithostratigraphy and Basin Structure of the Southern Karoo Basin Re-Visited.

10.1007/978-3-319-40859-0_1, pp. 3-16.

Mälicke, M., Hassler, S., Weiler, M., Blume, T. and Zehe, E. (2018). Exploring hydrological similarity during soil moisture recession periods using time dependent variograms. *Hydrology and Earth System Sciences Discussions*, [online] pp.1-25. https://www.researchgate.net/publication/327702704_Exploring_hydrological_similarity_during_soil_moisture_recession_periods_using_time_dependent_variograms.

Mariethoz, G., Renard, P., Cornaton, F. and Jaquet, O. (2009). Truncated Plurigaussian Simulations to Characterize Aquifer Heterogeneity. *Ground Water*, 47(1), pp.13-15.

Matheron, G. (1963). Principles of geostatistics. *Economic Geology*, 58(8), pp.1246-1266.

Mohaghegh, S., Gruic, O., Zargari, S., Dahaghi, A. and Bromhal, G. (2012). Top-down, intelligent reservoir modelling of oil and gas producing shale reservoirs: case studies. *International Journal of Oil, Gas and Coal Technology*, [online] 5(1), p.3.

Mosavel, H. and Musekiwa, C. (2016). 3D geology modelling from boreholes, crosssections and geological maps to support shale gas potential investigations in the Beaufort West area, South Africa. *International Geological Congress, Abstracts*, [online] Abstract 5498. http://0search.ebscohost.com.innopac.wits.ac.za/login.aspx?direct=true&db=geh&AN=2 017047686&site=eds-live&scope=site

Motherearthnews.com. (2012). *The Case for a Ban on Fracking*. [online] https://www.motherearthnews.com/nature-and-environment/environmental-policy/fracking-hydraulic-fracturing-zmgz12fmzrog.

Muntendam-Bos, A., Wassing, B., ter Heege, J., van Bergen, F., Schavemaker, Y., van Gessel, S., de Jong, M., Nelskamp, S., van Thienen-Visser, K., Guasti, E., van den Belt, F. and Marges, V. (2009). *Inventory non-conventional gas*. TNO-034-UT-2009-00774/B. [online] Netherlands: TNO, pp.101-121.

https://www.yumpu.com/en/document/read/7578523/inventory-non-conventional-gas-2009-ebn/155.

Nolte, S., Geel, C., Amann-Hildenbrand, A., Krooss, B. and Littke, R. (2019). Petrophysical and geochemical characterization of potential unconventional gas shale reservoirs in the southern Karoo Basin, South Africa. *International Journal of Coal Geology*, 212, pp.1-16.

Oliver, M. and Webster, R. (1990). Kriging: a method of interpolation for geographical information systems. *International journal of geographical information systems*, 4(3), pp.313-325.

Olson, B. (n.d.). *3D RESERVOIR MODELING PROJECTS*. [ebook] Texas, pp.1-9.

Pepper, A. (1991). Estimating the petroleum expulsion behaviour of source rocks: a novel quantitative approach. *Geological Society, London, Special Publications*, [online] 59(1), pp.9-31. https://sp.lyellcollection.org/content/59/1/9.

Pro.arcgis.com. (2019). *What is geostatistics?—ArcGIS Pro | ArcGIS Desktop*. [online] https://pro.arcgis.com/en/pro-app/help/analysis/geostatistical-analyst/what-is-geostatistics-.htm

Rowsell, D. and de Swardt, A. (1976). Diagenesis in Cape and Karroo sediments, South Africa, and its bearing on their hydrocarbon potential. *Trans. R. Soc. South Africa*, 79, pp.81-145.

Saikia, K., Ikuku, C. and Sarkar, B. (2017). An integrated approach to discretized 3D modeling of geomechanical properties for unconventional mature field appraisal in the western Canadian sedimentary basin. *Journal of Petroleum Exploration and Production Technology*, 8(2), pp.418-429.

Scheiber-Enslin, S., Webb, S. and Ebbing, J. (2014). Geophysically Plumbing the Main Karoo Basin, South Africa. *South African Journal of Geology*, 117(2), pp.275-300.

Schwarzkopf, T. (1992). Source rock potential (TOC + hydrogen index) evaluation by integrating well log and geochemical data. *Organic Geochemistry*, 19(4-6), pp.545-549.

Selley, R. (1998). *Elements of petroleum geology*. 2nd ed. USA: Academic Press.

Shafer, J. (2006). Conditional Simulation. *Encyclopedia of Environmetrics*, p.1.

Smith, R., 1990. A review of stratigraphy and sedimentary environments of the Karoo Basin of South Africa. *Journal of African Earth Sciences (and the Middle East)*, 10(1-2), pp.117-137.

Smithard, T., Bordy, E. and Reid, D. (2015). The Effect of Dolerite Intrusions on the Hydrocarbon Potential of the Lower Permian Whitehill Formation (Karoo Supergroup) in South Africa and Southern Namibia: A Preliminary Study. *South African Journal of Geology*, [online] 118(4), pp.489-510.

Steyl, G., van Tonder, G. and Chevallier, L. (2012). *State of the art: Fracking for shale gas exploration in South Africa and the impact on water resources.* [online] *Water Research Commission*, pp.7-20.
http://www.wrc.org.za/wp-content/uploads/mdocs/KV%20294-11.pdf.

Sunjay, S., Kumar, S. and Jain, N. (2014). Shale Gas: An Unconventional Gas Reservoir. *Research Gate,* [online]. Available at: https://www.researchgate.net/publication/263492317_Shale_Gas_An_Unconventional_Gas_Reservoir.

Usgs.gov. (2019). *What is hydraulic fracturing?*. [online] https://www.usgs.gov/faqs/what-hydraulic-fracturing?qt-news_science_products=0#qt-news_science_products

Wackernagel, H. (1995). Ordinary Kriging. In: H. Wackernagel, ed., *Multivariate Geostatistics*. Berlin: Springer, pp.74-81.

Wackernagel, H. (2013). *Basics in Geostatistics 3, Geostatistical Monte-Carlo methods: Conditional simulation*.

Wang, G. and Carr, T. (2013). Organic-rich Marcellus Shale lithofacies modeling and distribution pattern analysis in the Appalachian Basin. *AAPG Bulletin*, 97(12), pp.2173-2205.

Wopara, O. (2018). Technical and environmental issues in the production of unconventional shale gas resources. *Petroleum and Coal*, 60(6), pp.1050-1059.

Wright, M., Court, R., Kafantaris, F., Spathopoulos, F. and Sephton, M. (2015). A new rapid method for shale oil and shale gas assessment. *Fuel*, 153, pp.231-239.

YEW, C. (2017). *Mechanics of hydraulic fracturing*. 2nd ed. Massachusetts: Gulf Professional.

Zakrevsky, K. (2011). *Geological 3D modelling*. Houten: EAGE Publications.

Zhang, L., Shan, B., Zhao, Y., Du, J., Chen, J. and Tao, X. (2018). Gas Transport Model in Organic Shale Nanopores Considering Langmuir Slip Conditions and Diffusion: Pore Confinement, Real Gas, and Geomechanical Effects. *Energies*, 11(1), p.223.

APPENDICES

APPENDIX I

Calculations for Top Ecca Group to Top Whitehill Formation, and Whitehill and Prince Albert Formations using the AAPG volumetric calculation formula.

1. ***Top Ecca Group to Top Whitehill Formation***

SCENARIO 1

$$G = \frac{43560 \times 526\,042 \times 5026.25 \times 0.00095\ (0.1)}{0.00496}$$

= 2.206×10^{12} Scf

= 2.21 Tcf

SCENARIO 2

$$G = \frac{43560 \times 526\,042 \times 5026.25 \times 0.00856\ (0.5)}{0.00705}$$

= 6.992×10^{13} Scf

= 69.92 Tcf

SCENARIO 3

$$G = \frac{43560 \times 526\,042 \times 5026.25 \times 0.01667\ (0.9)}{0.006005}$$

= 2.878×10^{14} Scf

= 287.8 Tcf

2. *Whitehill and Prince Albert Formations*

SCENARIO 1

$$G = \frac{43560 \times 526\,042 \times 846.62 \times 0.00095\ (0.4)}{0.00378}$$

= 1.950×10^{12} Scf

= 1.95 Tcf

SCENARIO 2

$$G = \frac{43560 \times 526\,042 \times 846.62 \times 0.00856\ (0.75)}{0.00453}$$

= 2.749×10^{13} Scf

= 27.49 Tcf

SCENARIO 3

$$G = \frac{43560 \times 526\,042 \times 846.62 \times 0.01667\ (0.9)}{0.004155}$$

= 7.0049×10^{13} Scf

= 70.05 Tcf

APPENDIX II

Changing gas saturations

Top Ecca Group to Top Whitehill Formation

SCENARIO 1

$$G = \frac{43560 \times 526\,042 \times 5026.25 \times 0.00095\,(0.1)}{0.00496}$$

= 2.206×10^{12} Scf

= 2.21 Tcf

$$G = \frac{43560 \times 526\,042 \times 5026.25 \times 0.00095\,(0.5)}{0.00496}$$

= 1.103×10^{13} Scf

= 11.03 Tcf

$$G = \frac{43560 \times 526\,042 \times 5026.25 \times 0.00095\,(0.9)}{0.00496}$$

= 1.985×10^{13} Scf

= 19.85 Tcf

Changing porosity

Top Ecca Group to Top Whitehill Formation

SCENARIO 1

$$G = \frac{43560 \times 526\,042 \times 5026.25 \times 0.00095\,(0.1)}{0.00496}$$

= 2.206×10^{12} Scf

=2.21 Tcf

$$G = \frac{43560 \times 526\,042 \times 5026.25 \times 0.00856\,(0.1)}{0.00496}$$

= 1.988×10^{13} Scf

= 19.88 Tcf

$$G = \frac{43560 \times 526\,042 \times 5026.25 \times 0.01667\,(0.1)}{0.00496}$$

= 3.871×10^{13} Scf

= 38.71 Tcf